Elekofehinti *et al.*
Egyptian Journal of Medical Human Genetics (2025) 26:5
https://doi.org/10.1186/s43042-024-00625-z

Egyptian Journal of Medical Human Genetics

RESEARCH Open Access

Computer-guided identification of novel inhibitors of apoptosis-signaling kinase 1 from *Spondia mombim* bioactive compounds against colorectal cancer

Olusola Olalekan Elekofehinti[1,2], Hannah Oluwaseun Popoola[1], Adedotun Olayemi Oluwatuyi[1,2*], Opeyemi Iwaloye[1,2], Moses Orimoloye Akinjiyan[1,2], Oluwamodupe Cecilia[3], Frank Abimbola Ogundolie[4], Olalekan Isaac Olatunde[5], Oussama Abchir[6], Samir Chtita[6] and Joao Batista Texeira Rocha[7]

Abstract

Background Apoptosis-signaling kinase 1 is a MAPKKK (mitogen-activated protein kinase) overexpressed in various types of human cancer including colorectal cancer. It mediates inflammation and apoptosis and promotes cell proliferation through the transcription of cyclin D1. 5-Fluorouracil remains one of the primary recommended drugs to manage colorectal cancer. However, this drug often causes various adverse effects, notably diarrhea, vomiting, nausea, and leukopenia. Therefore, a novel treatment is required to eradicate these problems. The clinical implication of apoptosis-signaling kinase 1 in the pathogenicity of colorectal cancer makes it an important drug target in the treatment of colorectal cancer. The use of natural compounds in human cancer treatment continues to gain significant attention in the scientific community due to their therapeutic efficacy.

Method In this study, computational models such as flexible docking, induced fit docking, and binding free energy calculation were employed to identify small molecule inhibitors from known bioactive compounds of *Spondias mombin* in reference to 5-fluorouracil (Colorectal cancer standard drug) targeting apoptosis-signaling kinase 1.

Results Molecular docking studies identified 10 promising candidates which include uvaretin, rutin, isoquercitrin, ellagic acid, quercetin, linalool, acetyl eugenol, tangeretin (-)-catechin, and d-sorbitol based on their favorable binding affinity, with uvaretin having the best score (– 11.328 kcal/mol). The results were further validated with more dependable analysis such as induced fit docking and binding free energy calculation. These compounds showed modest indices for ADMET parameters. Molecular dynamic simulation validated ellagic acid and (-)-catechin with greater binding stability as leading compounds.

Conclusion These compounds showed improved flexible docking results and formed considerable stable interaction with the protein than 5-fluorouracil. They are non-carcinogenic. The oral bioavailability and toxicities of these compounds are promising as compounds obeyed the Lipinski rule of five. The constructed quantitative structure–activity relationship model with a trustworthy R^2 coefficient value supports the inhibition prowess of these compounds. The findings from this research confer that these compounds could be considered potent apoptosis-signaling kinase 1

*Correspondence:
Adedotun Olayemi Oluwatuyi
oluwatuyiao@futa.edu.ng
Full list of author information is available at the end of the article

Springer Open

© The Author(s) 2025. **Open Access** This article is licensed under a Creative Commons Attribution 4.0 International License, which permits use, sharing, adaptation, distribution and reproduction in any medium or format, as long as you give appropriate credit to the original author(s) and the source, provide a link to the Creative Commons licence, and indicate if changes were made. The images or other third party material in this article are included in the article's Creative Commons licence, unless indicated otherwise in a credit line to the material. If material is not included in the article's Creative Commons licence and your intended use is not permitted by statutory regulation or exceeds the permitted use, you will need to obtain permission directly from the copyright holder. To view a copy of this licence, visit http://creativecommons.org/licenses/by/4.0/.

inhibitors, and these could be confirmed experimentally as lead compounds of apoptosis-signaling kinase 1 inhibitors in colorectal cancer.

Keywords Colorectal cancer, ASK 1, Molecular docking, Novel inhibitors, *Spondias mombin*, 5-Fluorouracil

Introduction

Cancer is the uncontrolled growth of abnormal cells. When a cell gets damaged, it should undergo apoptosis, but the inability of the damaged cell to undergo apoptosis leads to uncontrolled cell division and growth. This growth can be benign which means it is just a tumor that grows locally and cannot metastasize [1]. When the growth is malignant, it means that the damaged cell can enter into the blood–lymph system and metastasize into other tissues, replicating uncontrollably in these new tissues and this is cancerous [2, 3]. According to GLOBOCAN 2020, cancer accounts for about 10 million deaths, and almost twice in diagnosis making it the main reason for global death. It is also predicted that by 2040 occurrence of cancer will increase to 28.4 million [4, 5].

Colorectal cancer (CRC) constituted 10% of the world's cancer incidence and 9.4% of all cancer-related deaths, in 2020. According to projections of aging, population expansion, and human progress, the number of new CRC cases worldwide is expected to reach 3.2 million in 2040 [6, 7]. CRC is a prevalent and lethal disease with metastasis being the major cause of death in the majority of individuals diagnosed. Common sites of distant metastasis are the liver and the peritoneum. [8, 9]. In regard to the epidemiology of cancer, the pathway of the cancer formation is a complex multistage process that involves consecutive mutational events that take place as cancer growth progresses [10]. All of this process leads to uncontrolled cell proliferation, angiogenesis, alleviation of apoptosis, malignancy, and multi-drug resistance in different cancers [11]. The progression of CRC is characterized by many molecular mechanisms, one of which is epidermal growth factor receptor (EGFR) over-expression, which takes part in many cellular processes that include growth, proliferation, and survival of normal cells [10, 12].

The JAK/STAT3 pathway, PI3K/AKT, RAS/RAF/MEK/ERK, and other downstream intracellular signaling pathways that control cell migration, proliferation, and survival are all activated by the EGFR pathway [13]. Specifically, the autophosphorylation on the tyrosine residues of EGFR triggers the signaling pathways in downstream of the Ras/Mitogen-activated protein kinases (MAPKs) [14]. MAPKs regulate numerous cellular activities, including proliferation, growth, migration, and apoptosis [15]. The Ser/Thr kinases family $MAPK_S$ trigger the many rounds of phosphorylation-activating kinases circles which is essential in the induction of cellular signaling [16]. Within the MAPKs family, ASK1 (also known as MEKK5) is recognized as an upstream kinase of the MKK4/7-JNK and MKK3/6-p38 pathways [17]. Apoptosis-signaling kinase 1 (ASK1) activates SEK1 and MAPK6 that then triggers the SAPK/c-Jun, N-terminal kinase (JNKs), and p38 MAPKs that induce programmed cell death [18]. Some cellular stress conditions, such as oxidative and endoplasmic reticulum stress, have been demonstrated in earlier research to activate ASK1, which is involved in intracellular stress and apoptotic signaling pathways [17], as shown in the pathway below (Fig. 1 [17]). Research has shown that osteosarcoma, breast, liver, lung, and colon cancer cells undergo apoptosis when ASK1 is activated [17, 19] ASK1 has been shown to stimulate tumor growth and cell proliferation in certain cancer types, including pancreatic, ovarian, and gastric malignancies [17, 20, 21]. A xenografted mouse model has demonstrated that the ASK1 inhibitor K811 suppresses the formation of gastric tumors [22, 23]. The binding of an inhibitor for the ASK 1 deactivation process is crucial for the regulation of ASK 1 activity in cancer cells [24].

This new perspective in the treatment of colorectal cancer is to target ASK-1, which signaling mechanism has been identified for regulation of cancer cell proliferation and migration.

The main therapeutic drug currently being utilized to treat CRC is 5-fluorouracil (5-FU), an intravenous synthetic fluorinated pyrimidine analog that must be converted intracellularly into active metabolites [25]. However, 5-FU has wide range of negative pharmacological effects. Diarrhea is the most often reported adverse reaction in patients receiving systematic 5-FU therapy. Dehydration, nausea, and vomiting are among the more typical side effects. Neutropenia, pyrexia, pulmonary embolism, thrombocytopenia, and leukopenia are more severe side effects that need to be addressed in individuals taking systemic 5-FU chemotherapy [26].

Plant secondary metabolites have been discovered to have great therapeutic use in curing different diseases [27]. Also, studies have shown that colorectal cancer can be treated with the use of plant secondary metabolites which could be the repair of damaged nucleic acids [23]. *Spondias mombin (S. mombin)* is a plant that is abundant in a wide range of secondary metabolites, such as phenolics, sterols, triterpenes, saponins, essential oils, amino acids, and polysaccharides [28]. *S. mombin* which

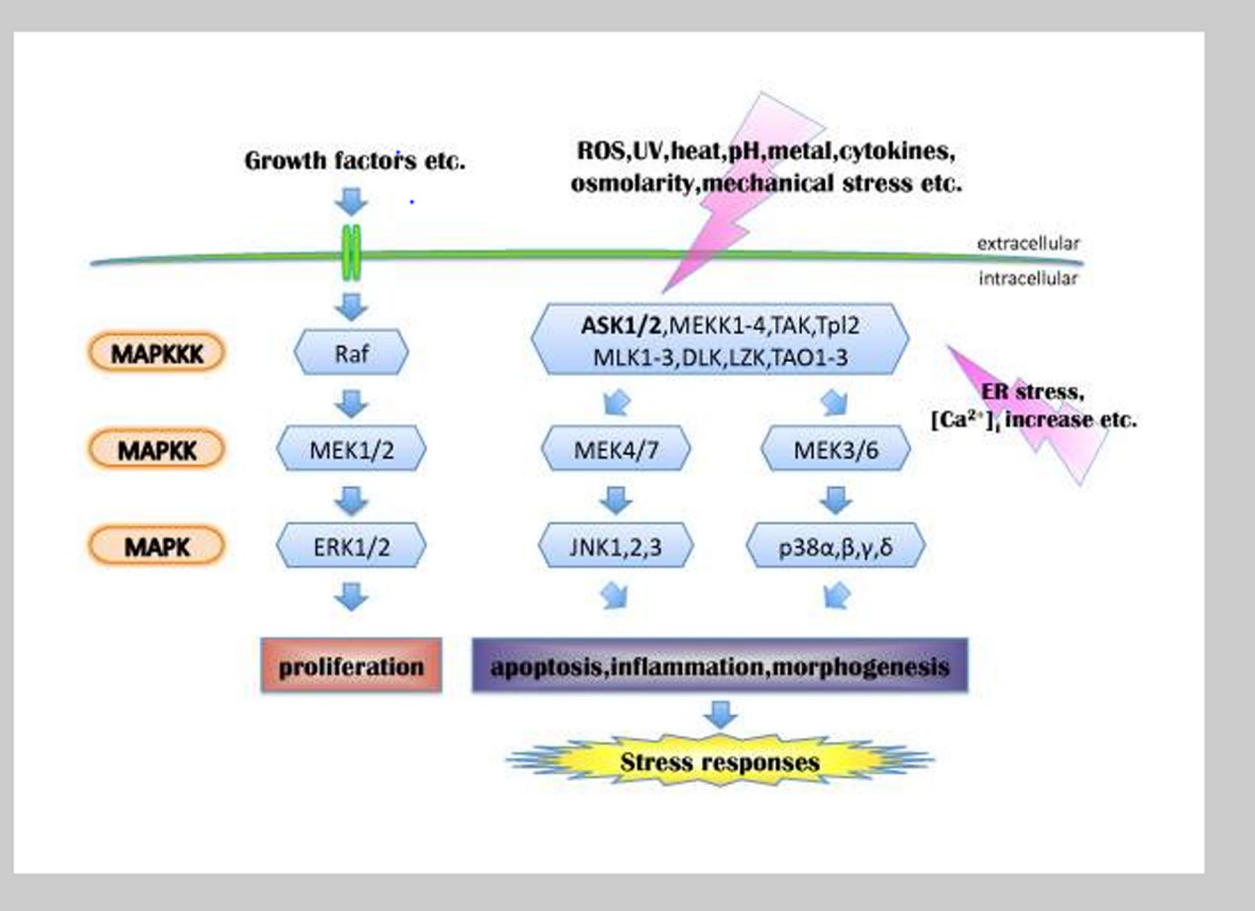


Fig. 1 A detailed cascade of MAPKs pathway in mammals. ASK1 and ASK2 belong to the MAPKKK family, which is responsible for initiating the MAPK cascade in response to various external leading to cell proliferation, apoptosis, inflammation, morphogenesis [17]

is popularly called Hog plum in the English language is an Anacardiaceae family, commonly found in tropical America, Nigeria, and Brazil, and other tropical rain forests [29, 30]. Different parts of *S. mombin* with significant phytochemicals have been shown to exhibit bioactivity in the treatment of cancer and can also be used to alleviate inflammation [31]. Evidentially, studies on *S. mombin* leaves have shown that they have sedative, antipsychotic, antiepileptic, anti-inflammatory, anti-α-amylase, and antileishmanial activity effects. They have also been shown to have antioxidant, anti-inflammatory, hepatoprotective, and proton pump inhibitory properties [32, 33]. In vitro studies has been employed to validate the antitumoral and antiangiogenic effects.

Therefore, for this present study using computational analysis which includes molecular docking, induced fit docking, ADME studies, MM/GBSA calculation, QSAR modeling, and Molecular Dynamic simulation, we aim to determine the molecular interaction, inhibitory potentials, and druggability of phytocompounds from *Spondias mombin* against ASK 1, a target protein in CRC for a novel therapeutic.

Methodology

Maestro Schrodinger Suites software was the computational software tool used for the present research work [34].

Crystal structure of preparation of starting structure

The X-ray crystallographic protein structure of apoptosis-signaling kinase-1 (ASK-1 [35]) with co-crystallized ligand (PDB code 4BHN) was downloaded from the Protein Data Bank http://www.rcsb.org/pdb. The protein preparation wizard of the glide software was used in the preparation of ASK-1 to add residues and hydrogen atoms that are missing due to X-ray crystallographic limitation [36]. Following protocol used by Iwaloye et al. [37], bonds and missing hydrogen atoms were added in the protein preparation wizard, the H-bond network was optimized using PROPKA [38], and OPLS3e force field

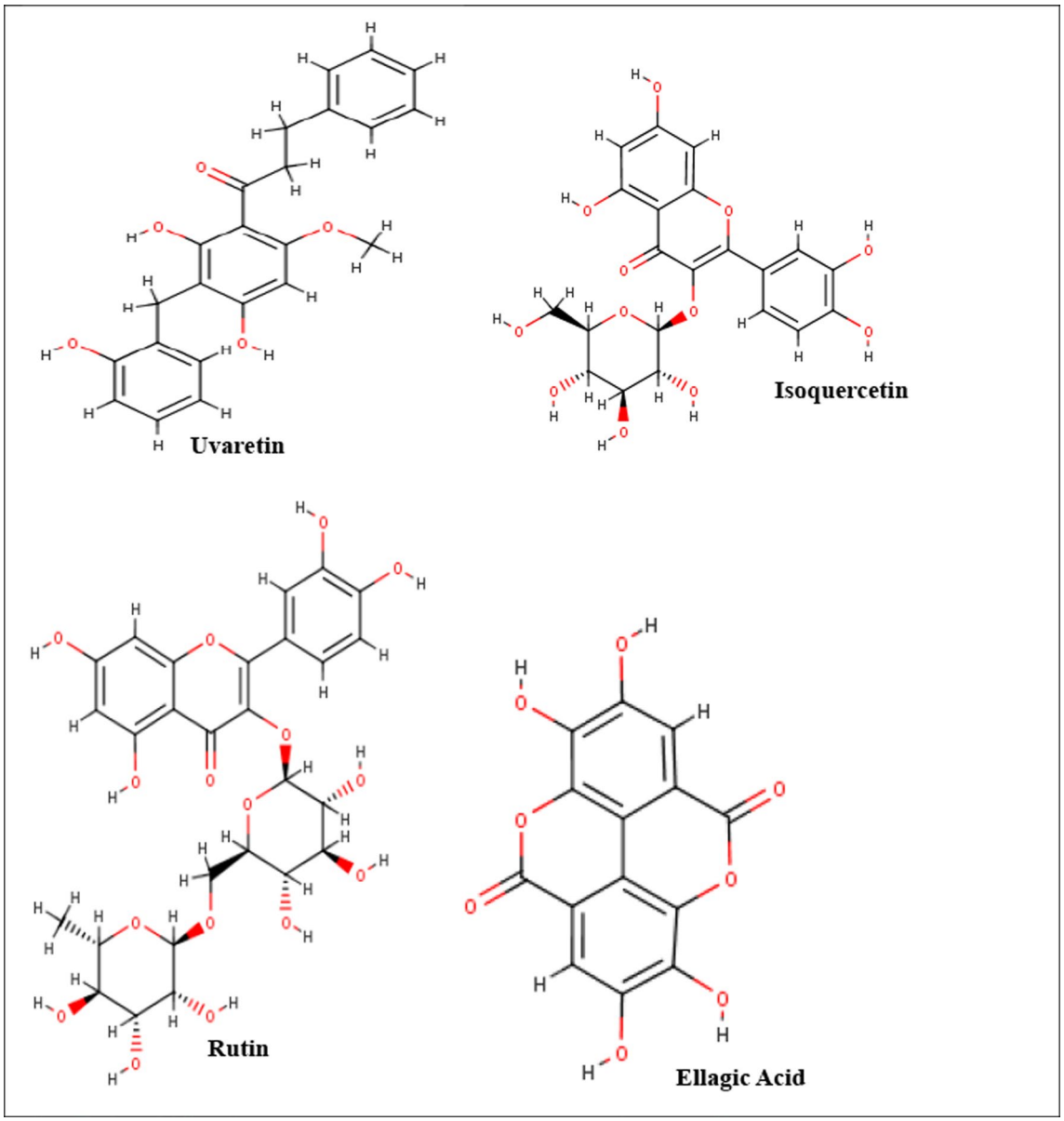


Fig. 2 2D structure of *Spondias mombin* promising compounds

was used to remove any steric hindrances in ASK 1 during the refinement step [39]. In order to have the x, y, and z coordinates supplied, Receptor Grid Generation was used to set up the glide grid file.

Library preparation of S. mombin phytochemicals

Phytochemical ligands of *S. mombin* were retrieved from the PubChem database https://pubchem.ncbi.nlm.nih.gov/ and loaded into Maestro using the Ligprep tool available in Schrodinger suites for molecular docking. This also generated a 3-dimensional ligand with adequate asymmetry (Ligprep, 2024) [40]. Epik v4.3 (Epik, 2024), OPLS3e force field was used in the generation of possible ionization states of each ligand structure at a physiological pH of 7 ± 2. All the other options were kept as default before energy minimization.

Pharmacokinetics profile prediction

Lipinski's rule of five was presumed by Canvas, and this was used in the determination of the ADMET properties and draggability of the phytochemicals in *S. mombin* [41, 42].

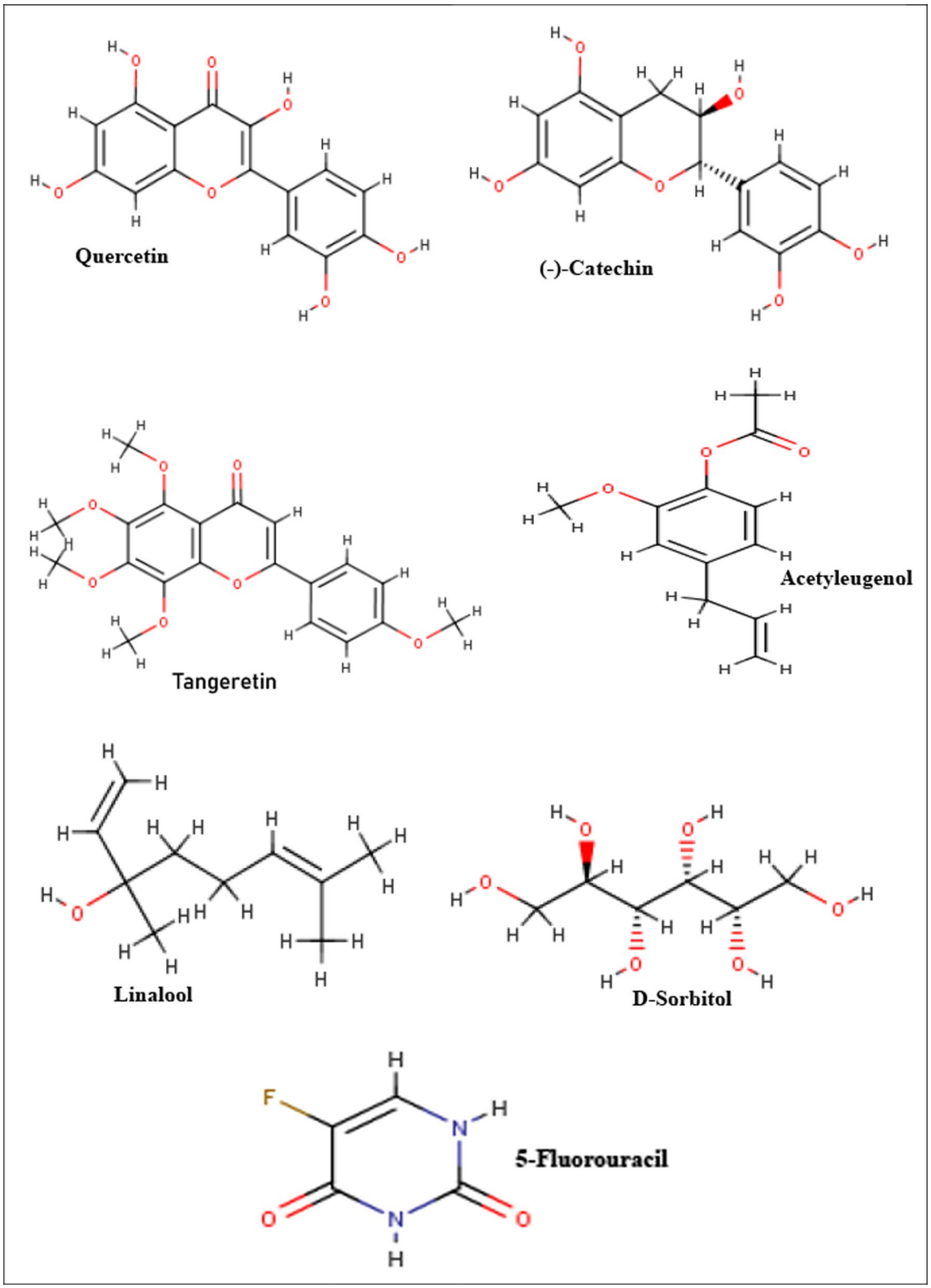


Fig. 2 continued

Table 1 Docking score, induced fit docking (IFD) score, and interacting residues, of the promising compounds of *S. mombin* and 5-fluorouracil with ASK-1 protein

Compounds name	Docking score (kcal/mol)	IFD score (kcal/mol)	Hydrophobic interaction
Uvaretin	− 11.328	− 548.79	Asp699, Asn702, Leu670, Leu671, Glu672, Tyr673, Tyr675, Phe753, Lys751, Phe749, Asn747, Glu746, Glu730, Phe744, Gly742, Leu741
Isoquercitrin	− 10.991	− 541.66	Phe753, Leu670, Leu671, Leu700, Lys751, Glu672, Thy673, Asp674, Tyr675, Asn747, Glu746, Phe744
Rutin	− 10.387	− 545.78	Ser701, Leu700, Asp699, Arg698, Ser743, Phe744, Glu746, Asn747, Phe753, Leu670, Leu671, Glu672, Tyr673, Asp674, Tyr673, Asp674, Tyr675
Ellagic acid	− 9.384	− 542.01	Glu672, Tyr675, Ser745, Phe744, Glu746, Asn747, Phe753
Quercetin	− 8.686	− 540.45	Leu670, Leu671, Glu672, Asp674, Tyr675, Gly742, Ser 743, Phe753, Phe744, Glu746, Lys751, Asn747
Catechin	− 8.017	− 514	Asp699, Leu700, Ser701, Leu,670, Leu671, Glu672, Tyr673, Tyr675, Phe744, Glu746, Asn747, Phe740, Lys751, Phe753
Tangeretin	− 7.943	− 535.17	Lys751, Phe753, Leu700, Ser743, Phe744, Glu746, Asn747, Leu671, Glu672, Tyr673, Asp674, Tyr675
Acetyl eugenol	− 6.49	− 535.12	Phe753, Lys751, Leu671, Glu672, Thr673, Tyr675, Ser743, Phe744, Glu746, Asn747, Ile708
Linalool	− 6.941	− 534.54	Leu700, Leu671, Glu672, Tyr673, Asp674, Tyr675, Tyr677, Phe753, Lys751, Ser743, Phe44, Glu746, Asn747
D-Sorbitol	− 6.434	− 534	Ser743, Phe744, Glu746, Asn747, Leu671, Tyr673, Tyr645, Phe753, Lys751
5-Fluorouracil	− 5.737	− 534.29	Leu810, Val7338, Val694, Ser821, Ala707, Lys709, Glu710, Phe744, Glu746, Phe749, Lys751, Phe753, Leu686, Met754, Glu755, Gln756, Tyr673, Tyr675, Leu810

Table 2 QikProp prediction of drug-likeness and ADME properties of the promising compounds of *S. mombin*

Compound name	mol[a] MW	Donor[b] HB	Acceptor[c] HB	Percent Human[d] Oral Absorption	RO5[e]
Uvaretin	634.46	11	19.3	0	3
Isoquercitrin	464.38	7	13.75	1.15	2
Rutin	610.52	9	20.55	0	3
Ellagic acid	302.2	4	8	35.55	0
Quercetin	302.24	4	5.25	52.76	0
(-)-Catechin	290.27	5	5.45	60.92	0
Tangeretin	268.27	0	3	100	0
linalool	378.42	2	4	100	0
Acetyl eugenol	206.24	0	3.25	100	0
D-Sorbitol	212.25	0	2	100	0

[a] Molecular weight of the molecule (range 130.0–725.0)

[b] Estimated number of hydrogen bonds that would be donated by the solute to water molecules in an aqueous solution (range 0.0–6.0)

[c] Estimated number of hydrogen bonds that would be accepted by the solute from water molecules in an aqueous solution (range 2.0–20.0)

[d] Percentage of human oral absorption (< 100%—> 20%)

[e] Lipinski rule of five (RO5) (Maximum violation: 3)

Determination of ligand binding site

The grid box for receptor binding was developed by determining the site where ligands bind in ASK 1 and the basis used for this was the site where the ligand was crystallized with the protein of interest (ASK 1) (4BHN), and this was used to assign the grid box for ligand binding that was at the center of coordinates ($x = 93.91$, $y = 68.0$, $z = 9.8$). The van der Waals radii of the receptor atoms with partial atomic charge were set to a scaling factor of 1.0 and partial cutoff of 0.25 to soften the potential for nonpolar parts of the receptor.

Table 3 *S. mombin* promising phytochemicals and 5-fluorouracil binding free energy against ASK-1

Compound name	ΔGBind[a]	ΔGBind[b] Coulomb	ΔG Bind[c] Solv GB	ΔGBind[d] Lipo	ΔGBind[e] H-bond
Uvaretin	− 91.21	− 43.16	38.76	− 37.61	− 2.48
Isoquercitrin	− 72.54	− 24.37	27.81	− 37.6	− 1.45
Rutin	− 60.99	− 28.4	31.95	− 31.26	− 1.21
Ellagic acid	− 72.67	− 15.49	16.65	− 30.91	− 1.44
Quercetin	− 64.87	− 28.99	28.13	− 29.38	− 2.11
(-)-Catechin	− 62.16	− 23.59	26.06	− 30.23	− 1.01
Tangeretin	− 65.69	− 17.21	15.87	− 33.62	− 0.66
Linalool	− 75.68	− 20.15	22.85	− 46.61	− 0.83
Acetyl eugenol	− 59.17	− 8.34	13.25	− 33.55	− 0.24
D-Sorbitol	− 60.78	− 7.8	10.43	− 30.22	− 0.25
5-Fluorouracil	− 33.8	− 12.66	7	− 8.25	− 0.5

[a] MM-GBSA free energy (kcal/mol) of binding

[b] Contribution to the MM-GBSA free energy of binding (kcal/mol) from the Coulomb energy

[c] Contribution to the MM-GBSA free energy of binding (kcal/mol) from solvent binding

[d] Contribution to the MM-GBSA free energy of binding (kcal/mol) from lipophilic binding

[e] Contribution to the MM-GBSA free energy of binding (kcal/mol) from hydrogen bonding

Molecular docking study

Ligands were docked with the glide standard precision (SP) docking initially, through the receptor grid file generated. The extra-precision (XP) docking was carried out to get more precise ligand poses, and this was done with the phytochemicals with the highest SP docking score [43]. Its scoring function is more accurate, sophisticated, and reliable when compared to SP.

MM-GBSA free energy calculation

Binding free energy was used to evaluate how stable the complex formed was so as to determine if the phytochemicals of S *mombin* with high docking score could block the ASK 1 activity. To solve for the binding free energy of compounds from *S. mombin* and ASK 1 complex, the Prime MM-GBSA was employed and this is based on the machinery embedded with Prime (2018) using OPLS3e force field and VSGB solvation model while setting every other thing to default, which then does the estimation of the difference in energy between the unbind and the bound Ask 1 complex after the energy minimization step, using the calculation for binding energy as previously described by [44].

Induced fit docking

To predict the affinity of the inhibitory phytochemicals of *S. mombin* to the prepared ASK 1 protein (4BHN) accurately, induced fit docking was carried out. Induced fit docking is a feature in the Glide/Refinement module in prime, and it is a computational tool that can reveal the conformational changes that occur as a result of ligands binding to the active site of a target protein receptor [45].

Phytochemicals of S mombin bioactivities predicted by QSAR modeling

The phytochemicals of *S. mombin* that have bioactivities that can inhibit ASK 1 were downloaded from the CHEMBL database https://www.ebi.ac.uk/chembl/. The phytochemicals alongside their inhibition constant (pIC50) were visualized using a text editor. AutoQSAR is a computational modeling tool that is embedded in the Schrödinger suite, it is an automated technology that assembles and employs the QSAR model, and this was used to develop the quantitative structure–activity relationship (QSAR) model which was eventually used to select the most favorable bioactive phytochemicals [46]. The structural data of *S. mombin* structure as the case may be along with its ADME properties are the input for AutoQSAR. It is an *in silico* method that enumerates unique fingerprints and descriptors. Ranking score, root-mean-square error (RMSE), standard deviation (SD), Q^2, and R^2 values are the calculations done after QSAR predictions [47].

Molecular dynamics

To evaluate the stability and viability of the predicted binding poses and interactions, molecular dynamics (MD) simulations were performed on the selected complexes [48–50]. Before initiating the MD simulations, the systems were prepared using the Preparation Wizard, which included deleting water molecules, adding hydrogen atoms, assigning bonds, performing energy minimization, and optimizing the structure of the complexes to ensure accurate simulation conditions [51]. The complexes were solvated and ionized in an orthorhombic

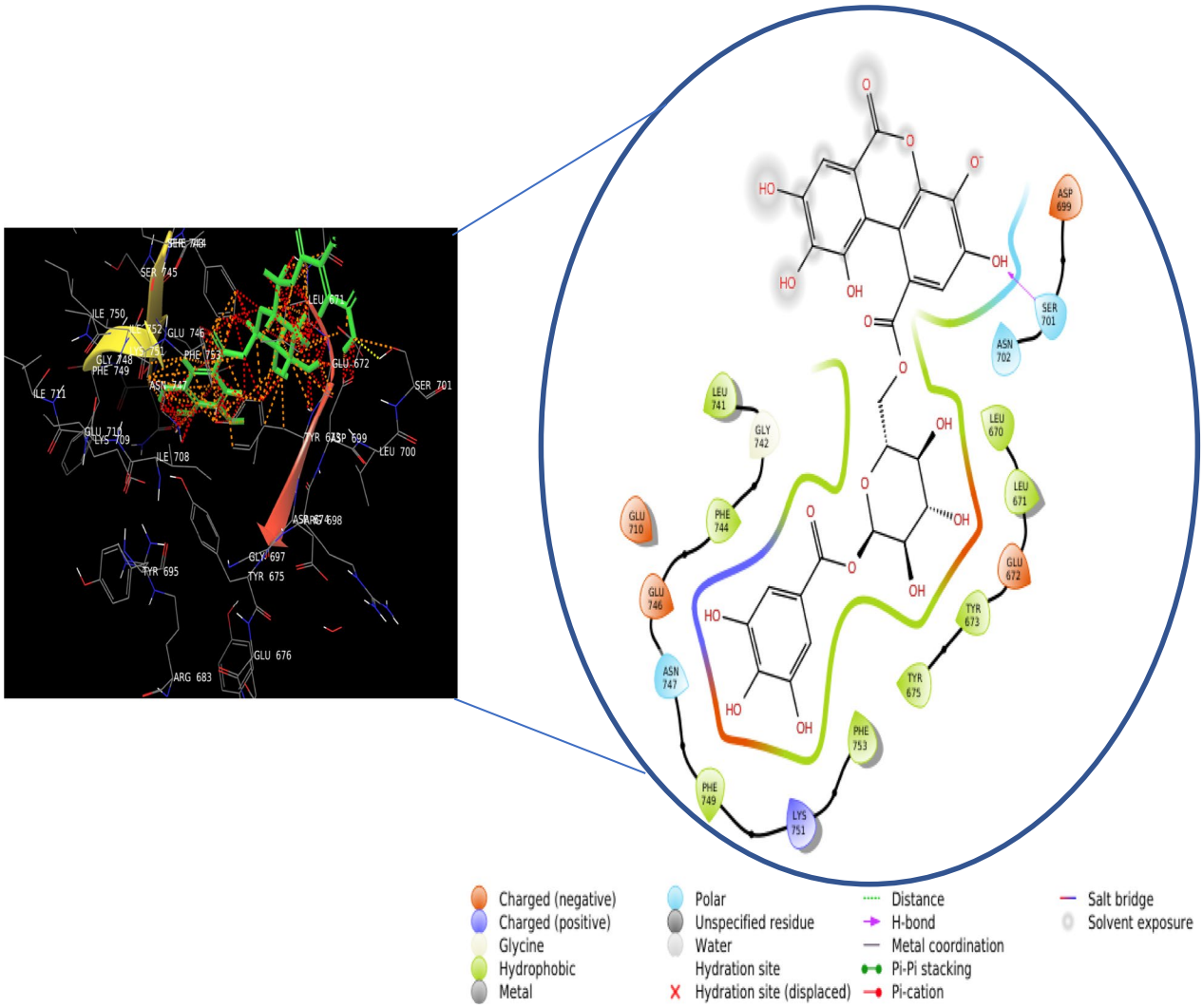


Fig. 3 Binding pose of uvaretin with apoptosis signal-regulating kinase 1 (ASK1) showing critical amino acid interaction within the protein's active site in 3D and 2D

box. TIP3P water molecules were used for solvation, while sodium and chloride ions were added to neutralize the systems. The prepared systems were equilibrated to stabilize them before running the MD simulations, ensuring that the environment was physiologically relevant for accurate interaction simulation [52, 53].

Using Desmond software, the MD simulations were first run for 1 ns under NVT conditions, followed by 100 ns under NPT conditions ($T = 300$ K, $P = 1.01325$ bar). The Nose–Hoover chain thermostat was applied to maintain temperature, while the Martyna–Tobias–Klein barostat was used to regulate pressure during the NPT simulations [54]. Parameters such as root-mean-square deviation (RMSD) and root-mean-square fluctuation (RMSF) were calculated throughout the entire simulation to assess the deviation and fluctuation of the protein. These values were plotted to visualize the stability of the system. Additionally, protein–ligand interactions were analyzed using contact histograms and timelines to evaluate the viability and strength of the resulting interactions [55]. In addition, ligand properties such as radius of gyration (Rg), solvent-accessible surface area (SASA), molecular surface area (MolSA), polar surface area (PSA), and intramolecular hydrogen bonds (intra HB) were also calculated to further assess the structural stability and interaction behavior of the ligands during the simulation.

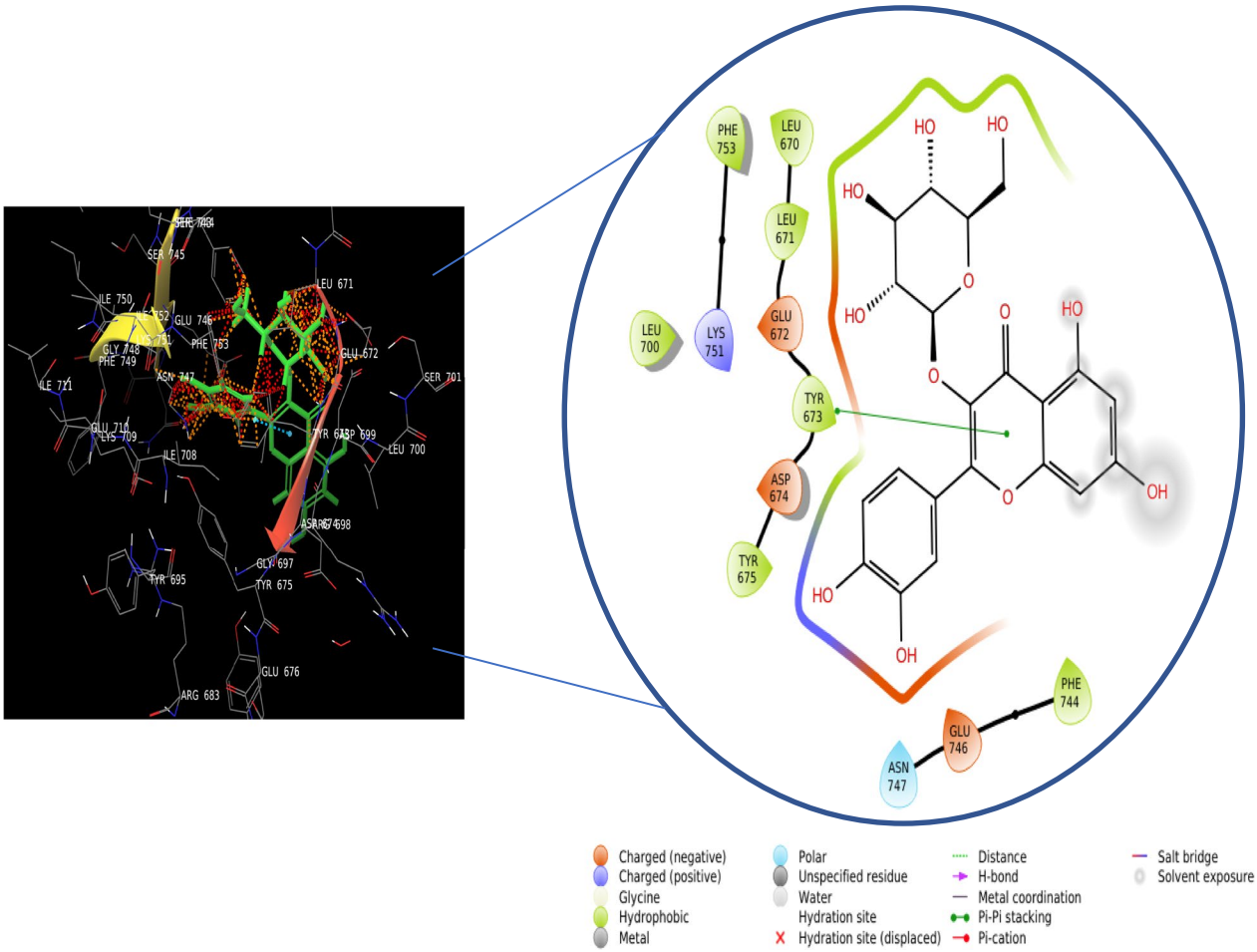


Fig. 4 Binding pose of isoquercitrin with apoptosis signal-regulating kinase 1 (ASK1) showing critical amino acid interaction within the protein's active site in 3D and 2D

Results

To identify the active compounds of S. mombin, the isolated compounds were first docked into the ASK-1 active site using standard precision. This led to the use of extra-precision (XP), a more accurate docking method [56]. These computational screenings of *Spondias mombin* compounds against ASK-1 implicated in colorectal cancer disease gave rise to ten [10] promising compounds. The ten promising compounds include uvaretin, rutin, isoquercitrin, ellagic acid, quercetin, linalool, acetyl eugenol, tangeretin catechin, and D-sorbitol; their 2D structure is displayed in Fig. 2, uvaretin had the most favorable docking score of − 11.328 kcal/mol; next in the docking score ranking are isoquercitrin and Rutin (− 10.991 kcal/mol and − 10.387 kcal/mol), respectively, compared to a reference ligand (5-Florouracil) with − 0.5.737 kcal/mol (Table 1). The induced fit docking analysis which further validates binding affinity of compounds to target revealed these compounds varying favorable scores better than 5-fluorouracil (standard drug) as shown in Table 1.

Table 2 depicts the 10 promising *S. mombin* compounds ADME and draggability properties, which included the molecular weight, Lipinski rule of 5 (RO5), as predicted by QikProp.

To confirm the binding stability and binding energy of the 10 promising compounds on active site of the target protein(ASK-1), prime MM-GBSA calculations was carried out [57]. The ten [10] natural products and ASK-1 complex were favorably stable with binding free energy (ΔGBind) scores which ranges from − 91.21 to − 60.78 kcal/mol in Table 3.

The binding poses of ASK-1 as shown in 2D and 3D (Figs. 3, 4, 5, 6, 7, 8, 9, 10, 11, 12 and 13) contain a range of amino acids, each of which interacts differently with the 10 hit phytochemicals and the reference ligand (5-fluorouracil) (Table 1). Hydrophobic interactions, pi–pi stacking, and H-bonding are a few examples of these

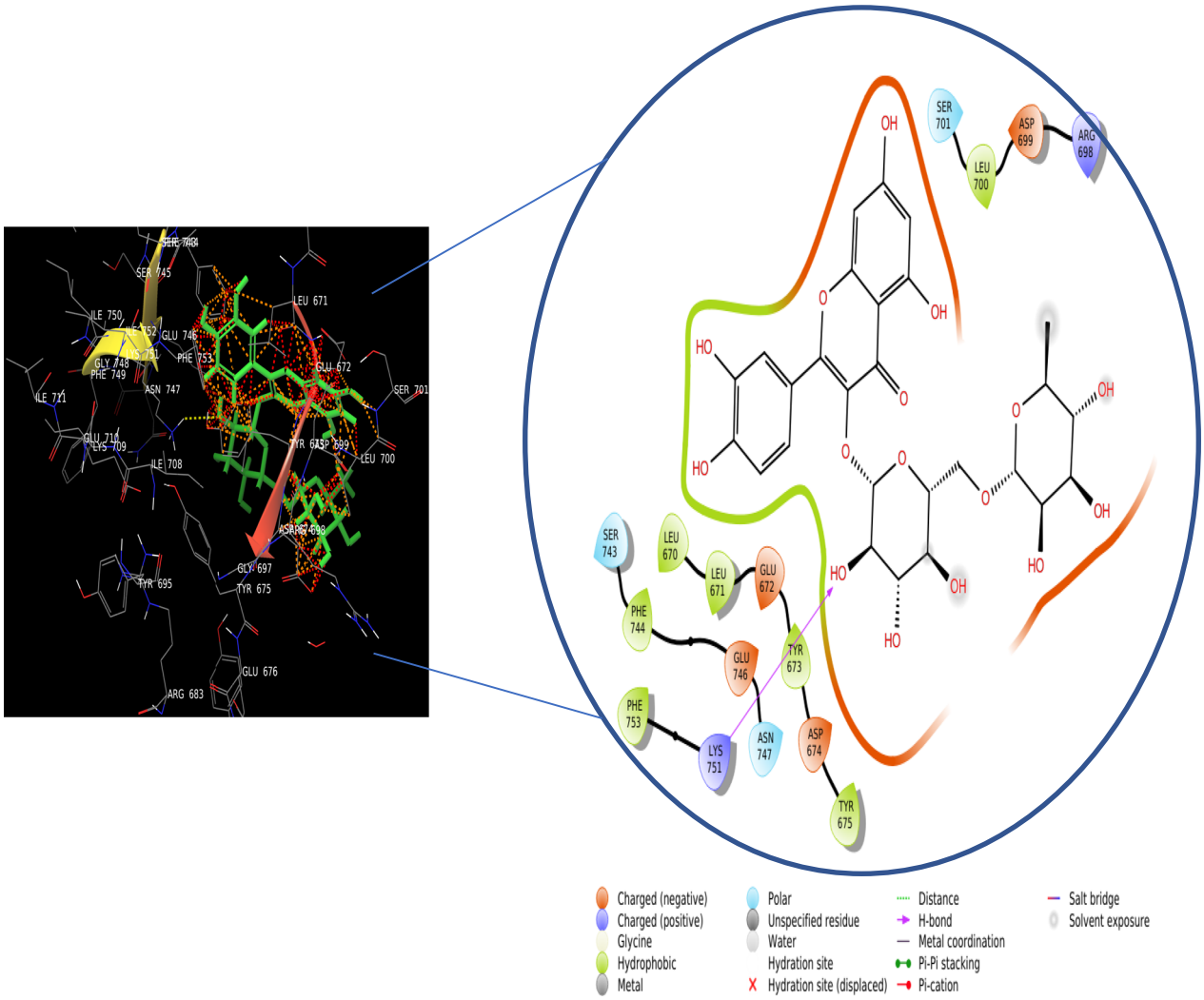


Fig. 5 Binding pose of rutin with apoptosis signal-regulating kinase 1 (ASK1) showing critical amino acid interaction within the protein's active site in 3D and 2D

interactions as shown in the legend of Figs. 3, 4, 5, 6, 7, 8, 9, 10, 11, 12 and 13.

The AutoQSAR tool randomly splits the experimental compounds into 75% training set and 25% test set and predicted activity of experimental compounds and observed activity by predicted model. The model was designed by using a non-linear method called kernel partial least square regression (KPLS) with fingerprint MOLPRINT2D used as a descriptor, with analysis of the best model kpls_desc_36 predicted by AUTOQSAR. Table 4 depicts QSAR model constructing parameters; R^2 of 0.8032; root-mean-square error (RMSE) of 0.5696; and Q^2 of 0.8028. The promising bioactive phytochemicals of *S. mombin* and its corresponding docking score and inhibitory values (pIC50) against ASK 1 as determined by QSAR models are also shown in Table 5. The AutoQSAR correlated the observed and anticipated pIC50 in a regression plot (Fig. 14).

Molecular dynamics simulations were conducted for the promising complexes. However, only the RMSD values of ellagic acid and catechin remained stable throughout the entire simulation period, indicating that no significant structural changes occurred in the receptor. This stability suggests that the binding of the ligands did not induce any major conformational shifts in the protein, which supports the robustness and reliability of the protein–ligand complexes. The calculated RMSD and RMSF parameters for the best two complexes, ellagic acid and catechin, are plotted in Figs. 15, 16 and 17 to facilitate the analysis of structural changes in the complexes throughout the simulation period. Figure 15 displays the RMSD profiles of the protein complexed with both selected compounds,

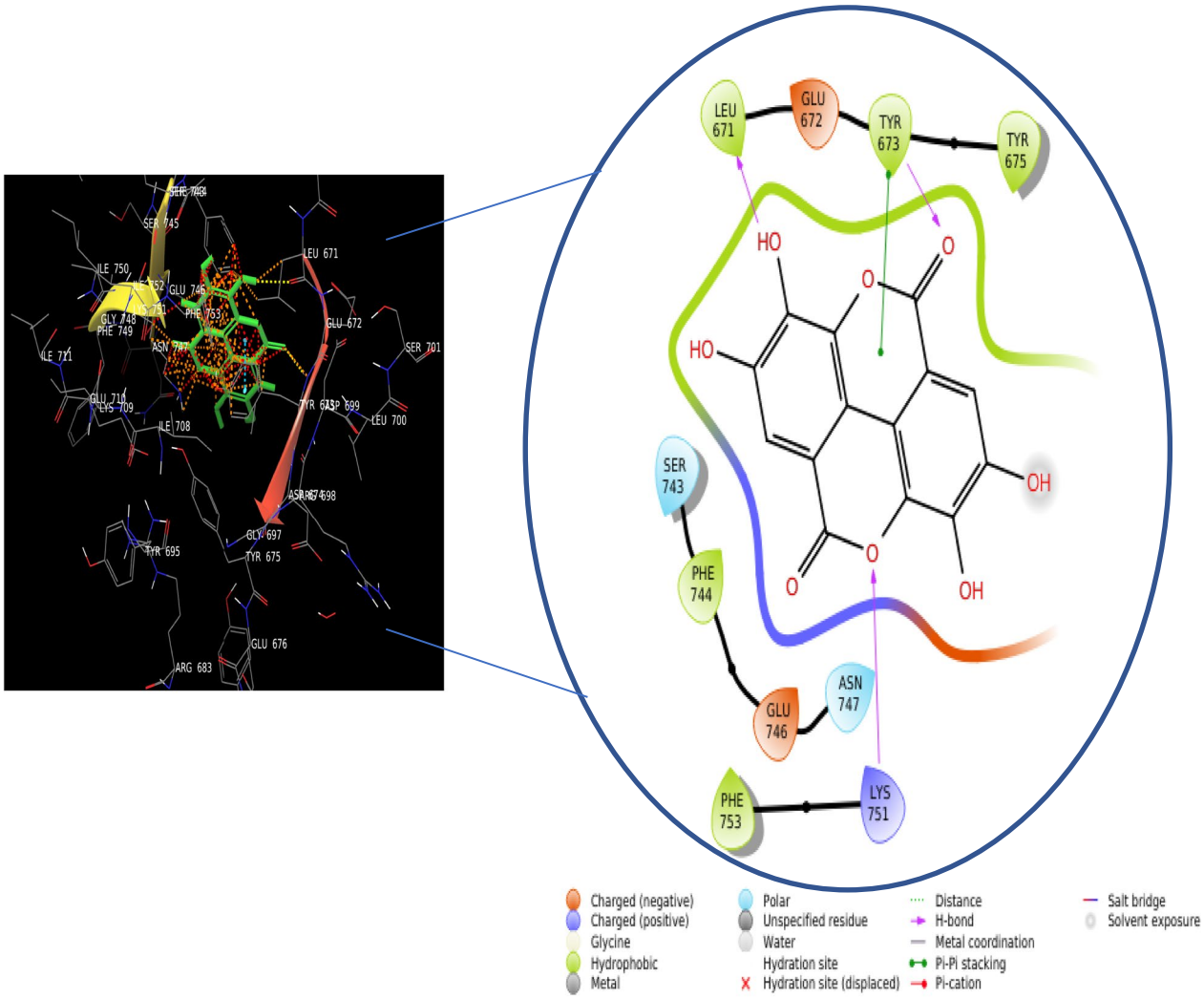


Fig. 6 Binding pose of ellagic acid with apoptosis signal-regulating kinase 1 (ASK1) showing critical amino acid interaction within the protein's active site in 3D and 2D

ellagic acid and catechin. The RMSD of the ligands in both complexes was also calculated (Fig. 16), revealing significant deviations, with RMSD values reaching 6 Å for catechin and 9 Å for ellagic acid. Additionally, the RMSF plot for the protein in both complexes showed minor fluctuations across most residues, except for Leu670, which exhibited a significant fluctuation of 5 Å, and Glu746, which displayed a moderate fluctuation of 3 Å (Fig. 17). The simulated complexes revealed the persistence of multiple interactions, including hydrophobic, hydrogen, and ionic bonds, as well as water bridges (Fig. 18). In the ellagic acid-4HBN complex, strong hydrogen bonds were observed with Glu672 and Asp699, along with three hydrophobic interactions involving Tyr673, Phe744, and Phe753. Additionally, water bridges were detected, highlighting further stabilization. In contrast, the catechin-4hbn complex displayed robust interactions, including hydrogen bonds with Leu670 and Glu746, as well as hydrophobic interactions with Leu671, Phe744, and Phe753. Water bridges involving Leu741, Leu670, and Leu671 were also detected.

During the simulation, various parameters were calculated and are illustrated in Fig. 19 to assess the structural changes associated with the ligands.

Discussion

Studies of colorectal cancer have become very popular but the therapeutic treatment is still very much limited as the death rate keeps increasing [58]. The available treatment for colorectal cancer is radio and chemotherapy alongside drugs like 5-fluorouracil, which has proven to generate reactive oxygen species which is detrimental to the health and leads to damage of the DNA which makes

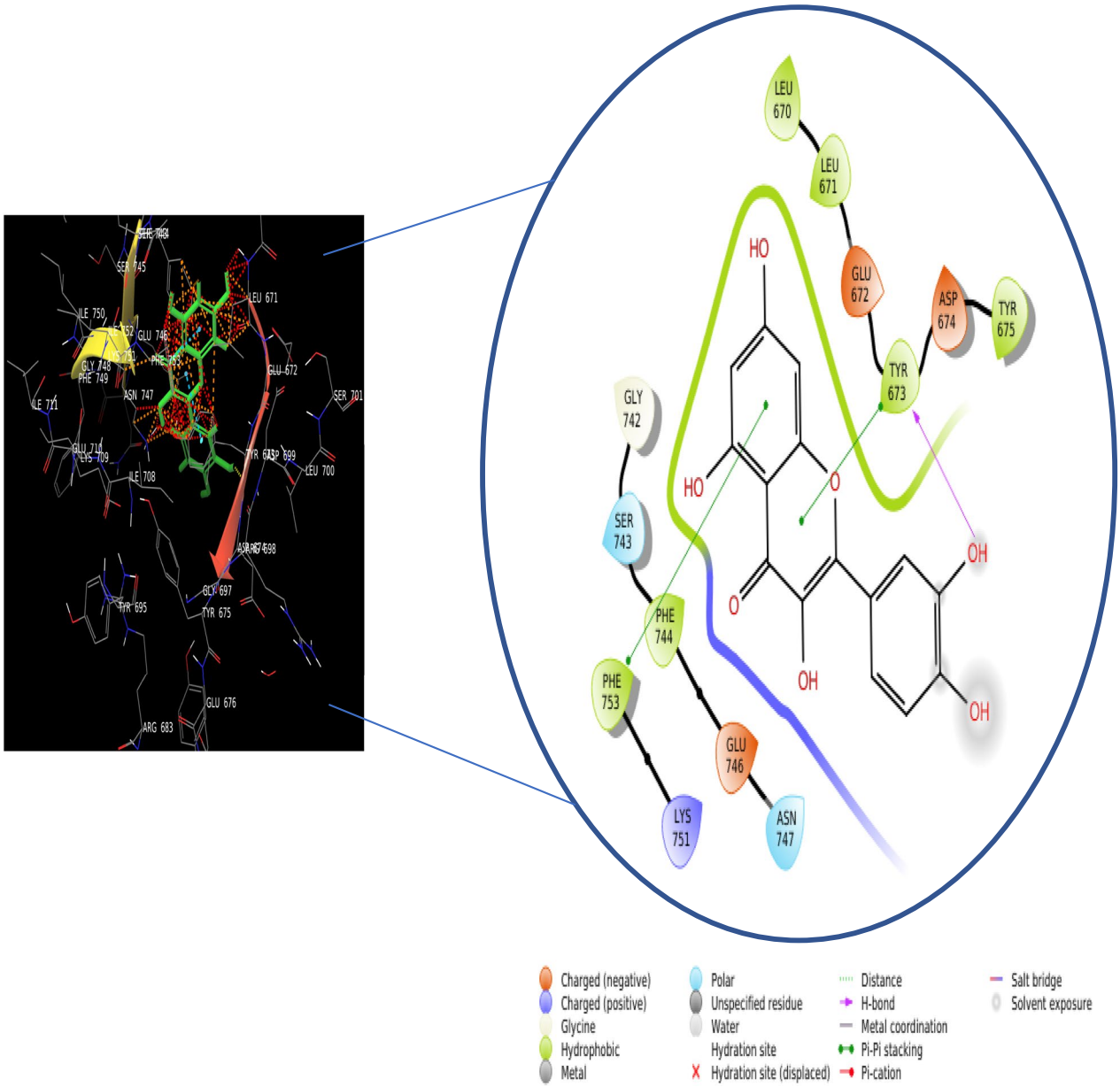


Fig. 7 Binding pose of quercetin with apoptosis signal-regulating kinase 1 (ASK1) showing critical amino acid interaction within the protein's active site in 3D and 2D

the treatment less effective [59], so there is a rising need for treatment with natural products such as plants secondary metabolites [60].

Conformational changes that occur when nascent discovered phytochemicals bind at the active site of target proteins leading to activation and deactivation of the activity the target can be determined using molecular computational modeling methods [61]. High negative value in terms of docking score shows most favorable interaction of ligand–protein complex [62]. In this study, the docking score of the 10 promising *S mombin* phytochemicals ranges from − 11.328 and − 6.434 kcal/mol compared to a reference ligand (5-Florouracil) with − 0.5.737 kcal/mol highlighting their potential as inhibitors for the target protein in the treatment of colorectal cancer.

Pharmacokinetics profile screening of plants secondary metabolites helps to screen out undruggable molecules and helps to overcome a hurdle in drugs discovery clinical trials stage [63, 64]. Druggability is a qualitative

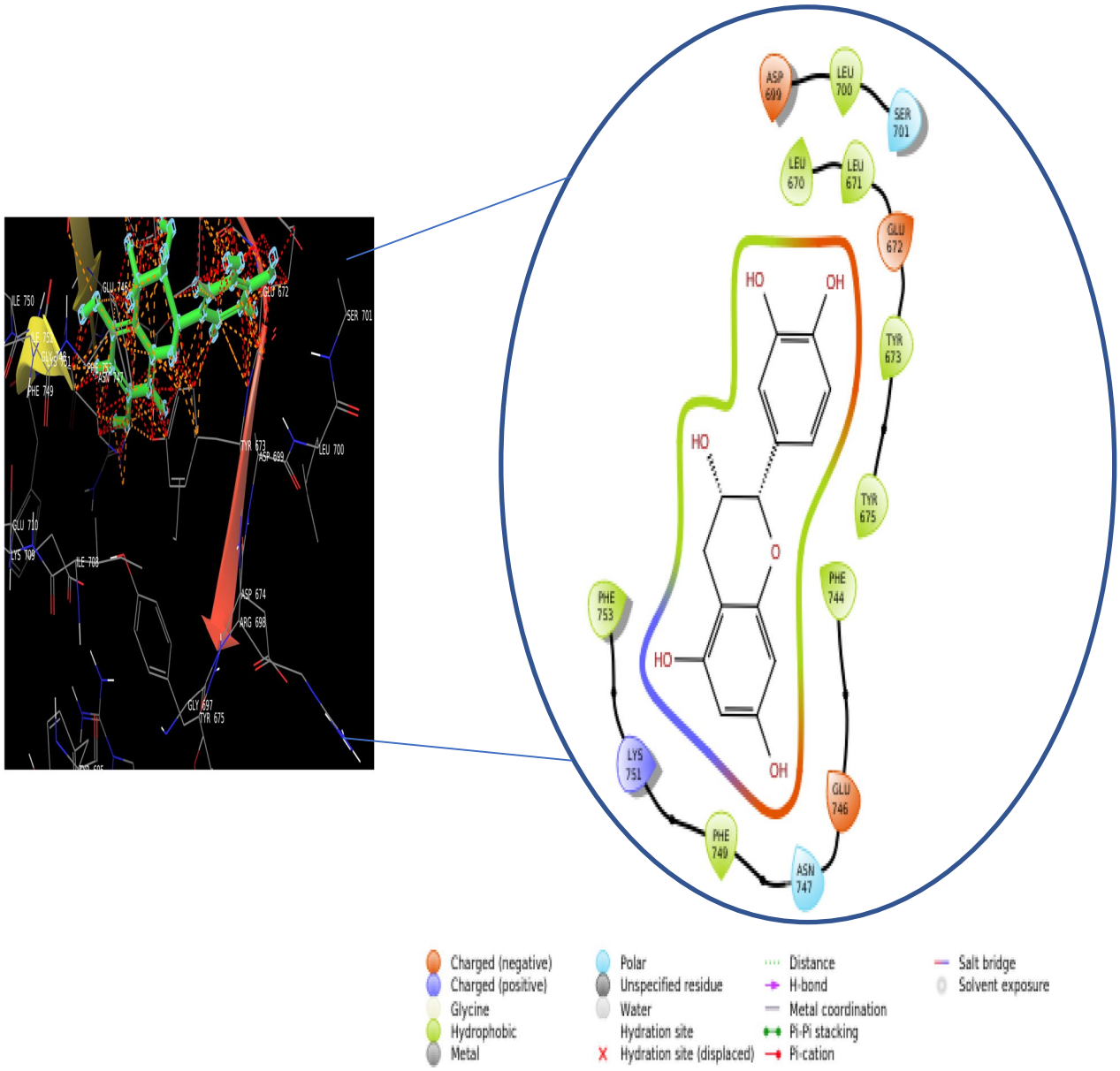


Fig. 8 Binding pose of catechin with apoptosis signal-regulating kinase 1 (ASK1) showing critical amino acid interaction within the protein's active site in 3D and 2D

measure of oral bioavailability that is determined by chemical structures and physicochemical features. The RO5 and percentage human oral absorption were adopted to predict the draggability of the promising phytocompounds as shown in Table 2. It may be concluded from the results that the majority of the substances, including D-sorbitol, acetyl eugenol, tangeretin (-)-catechin, ellagic acid, quercetin, linalool, and isoquercitrin, did not break Lipinski's rule of five and could be considered as orally absorbed agents. However, rutin and uvaretin violated the rule and may mostly be due to their high molecular weight. Since oral absorption of these two inhibitors may not be the best choice, alternative routes of absorption may be considered.

Coulomb interaction, covalent bond, lipophilic energy, and hydrogen bond energy from the MM-GBSA result contributed primarily to the binding free energy and thereby enhancing the activity of *promising compounds* to ASK-1 active site [65]. The more negative the values, the better the binding free energy and stability of the ligand in the active site of the target, Table 3 shows that uvaretin 1 binding to ASK-1 active site is the most stable,

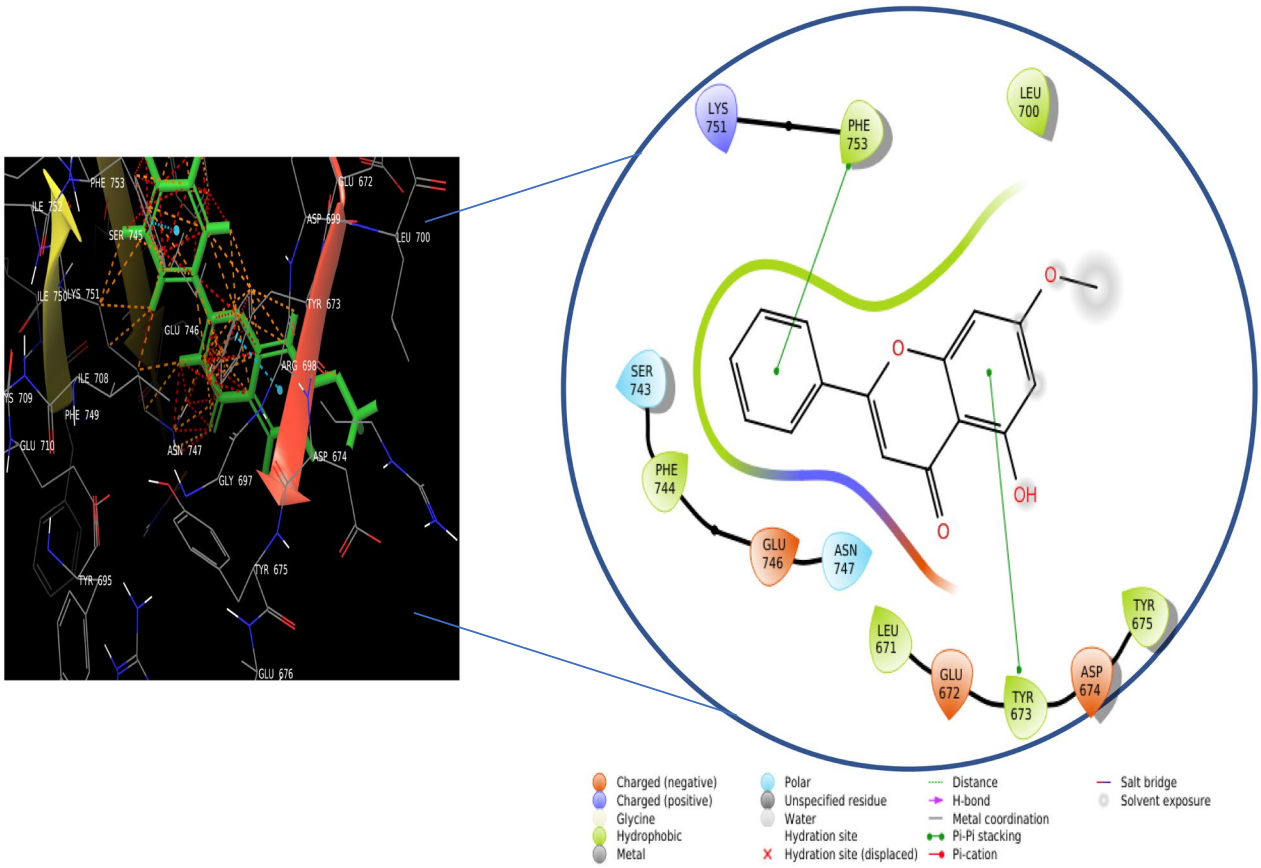


Fig. 9 Binding pose of tangeretin with apoptosis signal-regulating kinase 1 (ASK1) showing critical amino acid interaction within the protein's active site in 3D and 2D

while acetyl eugenol 1 interaction with ASK 1 active site is the lease stable.

The 2D structure (Figs. 3, 4, 5, 6, 7, 8, 9, 10, 11, 12 and 13) showing the binding pose of each hit ligand with ASK 1 had common amino acid residues which are as follows LEU670, LEU671, GLU672, TYR673, TYR675. PHE753, LYS751, ASN747, and PHE744. The post-docking analysis showed that uvaretin 1 formed one hydrogen bond with SER701, and rutin formed one hydrogen bond with LYS751. Ellagic acid formed three hydrogen bonds with LYS751, TYR673, and LEU671, and quercetin formed one hydrogen bond with TYR673. Isoquercitrin, ellagic acid, and tangeretin formed pi–pi stacking with TYR673 and tangeretin formed additional pi–pi stacking with PHE753, all of which facilitates the binding affinity and stability of each compound in the active site of the protein. All the promising compounds showed a very moderate pIC50 values as shown in Table 3, showing that they have the highest inhibitory effect of ASK-1.

The RMSD values remained stable throughout the entire simulation period, indicating that no significant structural changes occurred in the receptor. This stability suggests that the binding of the ligands did not induce any major conformational shifts in the protein, which supports the robustness and reliability of the protein–ligand complexes. These higher RMSD values indicate considerable movement of the ligands within the binding site over the course of the simulation. Such deviations suggest that the ligands may not have remained firmly anchored in a single binding pose, potentially exploring multiple orientations or conformations within the binding pocket. This could imply flexibility in the ligand–receptor interactions, which may influence the overall binding stability.

The fluctuations in the RMSF plot could be attributed to interactions between the ligands and these specific residues, suggesting that the binding of the ligands may have induced localized flexibility or movement in the protein structure, particularly in these regions. The higher fluctuation at Leu670 might indicate a more dynamic interaction, while the moderate fluctuation at Glu746 suggests a less pronounced, but still notable, effect of the ligand binding.

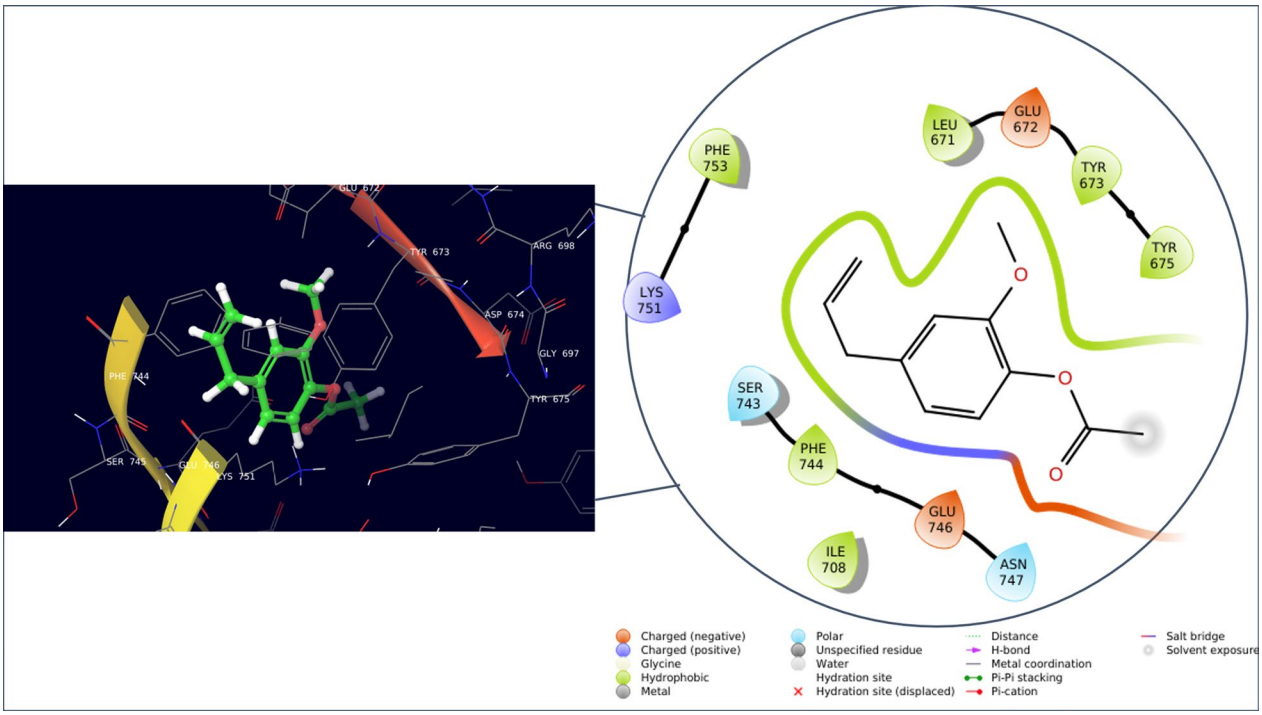


Fig. 10 Binding pose of acetyl eugenol with apoptosis signal-regulating kinase 1 (ASK1) showing critical amino acid interaction within the protein's active site in 3D and 2D

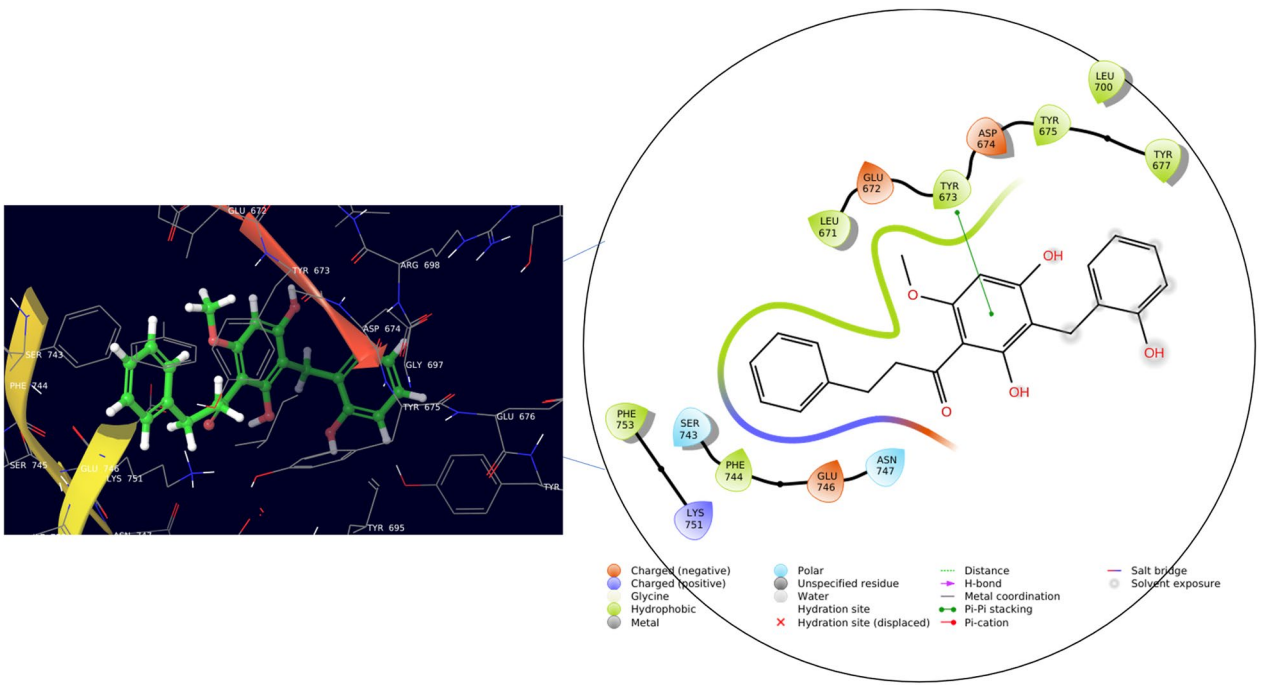


Fig. 11 Binding pose of linalool with apoptosis signal-regulating kinase 1 (ASK1) showing critical amino acid interaction within the protein's active site in 3D and 2D

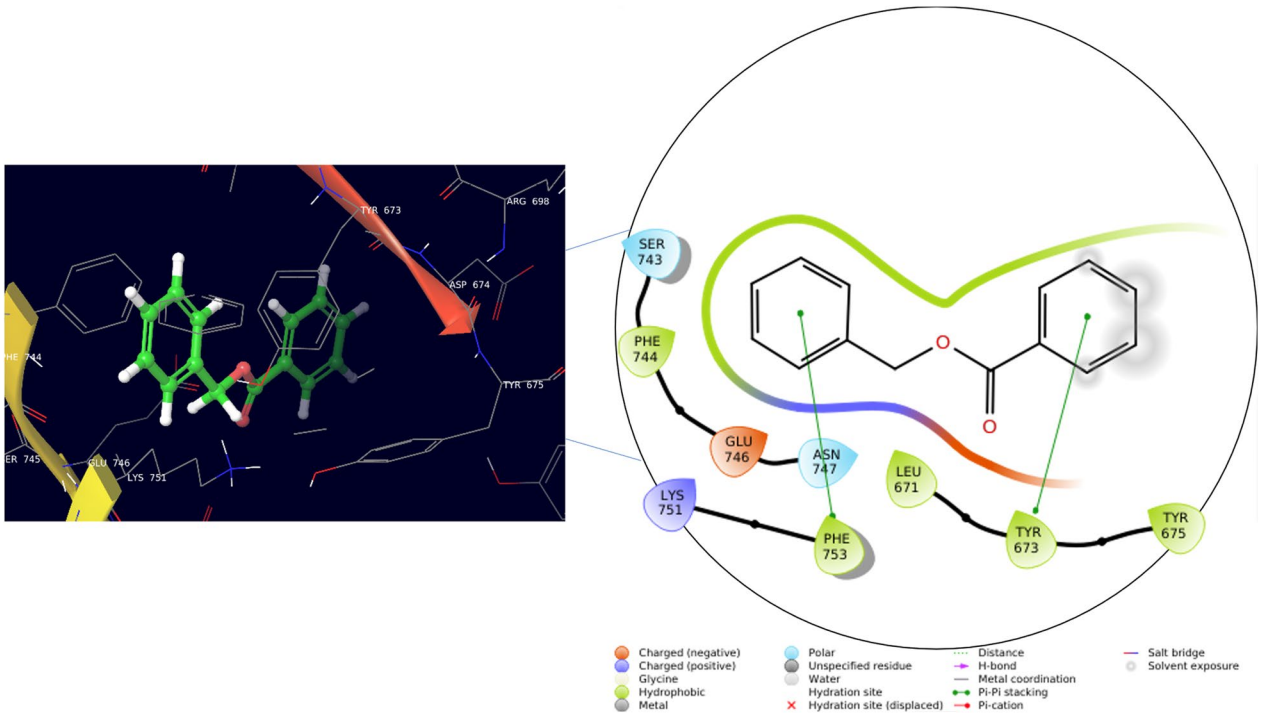


Fig. 12 Binding pose of D-sorbitol with apoptosis signal-regulating kinase 1 (ASK1) showing critical amino acid interaction within the protein's active site in 3D and 2D

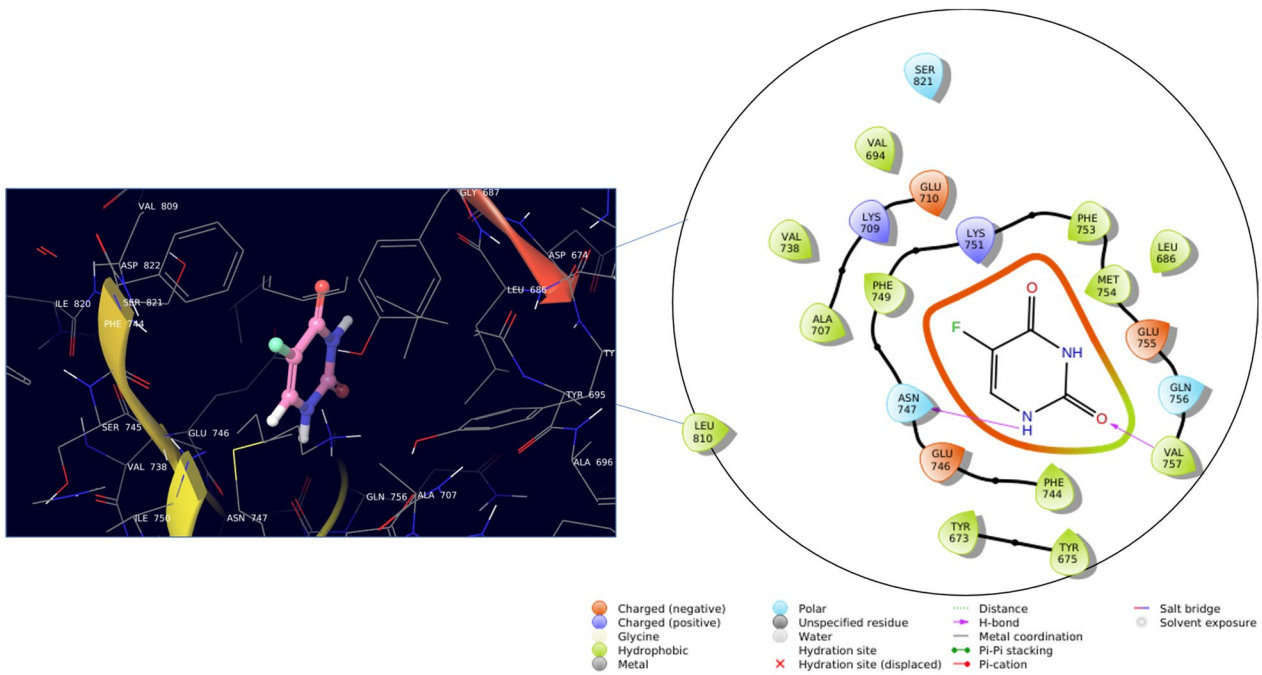


Fig. 13 Binding pose of 5-fluorouracil with apoptosis signal-regulating kinase 1 (ASK1) showing critical amino acid interaction within the protein's active site in 3D and 2D

Table 4 AUTOQSAR parameter corresponding to foremost model

Model code	Score	SD	R^2	RMSE	Q^2
kpls_desc_36	0.798532	0.5864	0.8032	0.5696	0.8028

Table 5 Promising compounds of *S. mombin* with their corresponding docking scores and inhibitory values (predicted PIC50)

Compounds name	Docking score (kcal/mol)	Predicted pIC50
Uvaretin	− 11.328	5.31
Isoquercitrin	− 10.991	4.56
Rutin	− 10.387	5.45
Ellagic acid	− 9.384	3.45
Quercetin	− 8.686	3.6
(-)-Catechin	− 8.017	3.83
Tangeretin	− 7.943	4.29
Acetyl eugenol	− 6.49	4.32
Linalool	− 6.941	4.37
D-Sorbitol	− 6.434	5.16
5-Fluorouracil	− 5.737	3.333

The protein–ligand interactions suggest that both ligands form a network of stable contacts with key residues, contributing to the overall stability of the complexes throughout the simulation. These interactions were consistently observed in both the timeline and the protein–ligand contact histogram.

For catechin, the radius of gyration initially started at 3.8 Å in the first 25 ns, decreasing slightly to 3.75 Å, where it remained until the end of the simulation. This gradual reduction suggests a minor compaction in catechin's structure, stabilizing over time. The molecular surface area stayed around 256 $Å^2$, indicating a consistent overall molecular exposure. Similarly, the polar surface area remained steady at 247 $Å^2$, reflecting stable polar interactions throughout the simulation. The solvent-accessible surface area displayed fluctuations between 60 and 180 $Å^2$, indicating that catechin's interactions with the surrounding solvent varied. These fluctuations likely resulted from conformational changes and dynamic interactions with the environment due to the flexibility of the catechin molecule.

For ellagic acid, all parameters demonstrated stability over the course of the simulation. The Rg stabilized at 3.27 Å, suggesting a compact and consistent structure. The MolSA remained stable at 231 $Å^2$, indicating that the overall molecular exposure did not change significantly. The SASA stabilized around 170 $Å^2$, suggesting limited fluctuations in solvent interactions. The PSA remained at 304 $Å^2$, reflecting a consistent exposure of the polar regions, which likely contributed to stable interactions with the solvent throughout the simulation. Finally, no intramolecular hydrogen bonds were detected for both systems.

The MD simulation demonstrated that catechin underwent minor structural adjustments, while ellagic acid exhibited greater structural stability. Both ligands maintained consistent surface properties, with catechin showing dynamic solvent interactions and ellagic acid remaining more structurally rigid.

Conclusion

The 10 potential compounds in this present investigation meet improved criteria as an ASK-1 inhibitor. All except rutin and uvaretin, in which another route of absorption should be used, have favorable oral absorption in humans. They demonstrated good docking scores compared to 5-fluorouracil and exhibit outstanding characteristics as potential drug candidates. However, Molecular Dynamic simulation drug further validated catechin and ellagic acid. We therefore, propose future in vivo and in vitro studies with these promising compounds to further prove their inhibitory activities of ASK-1.

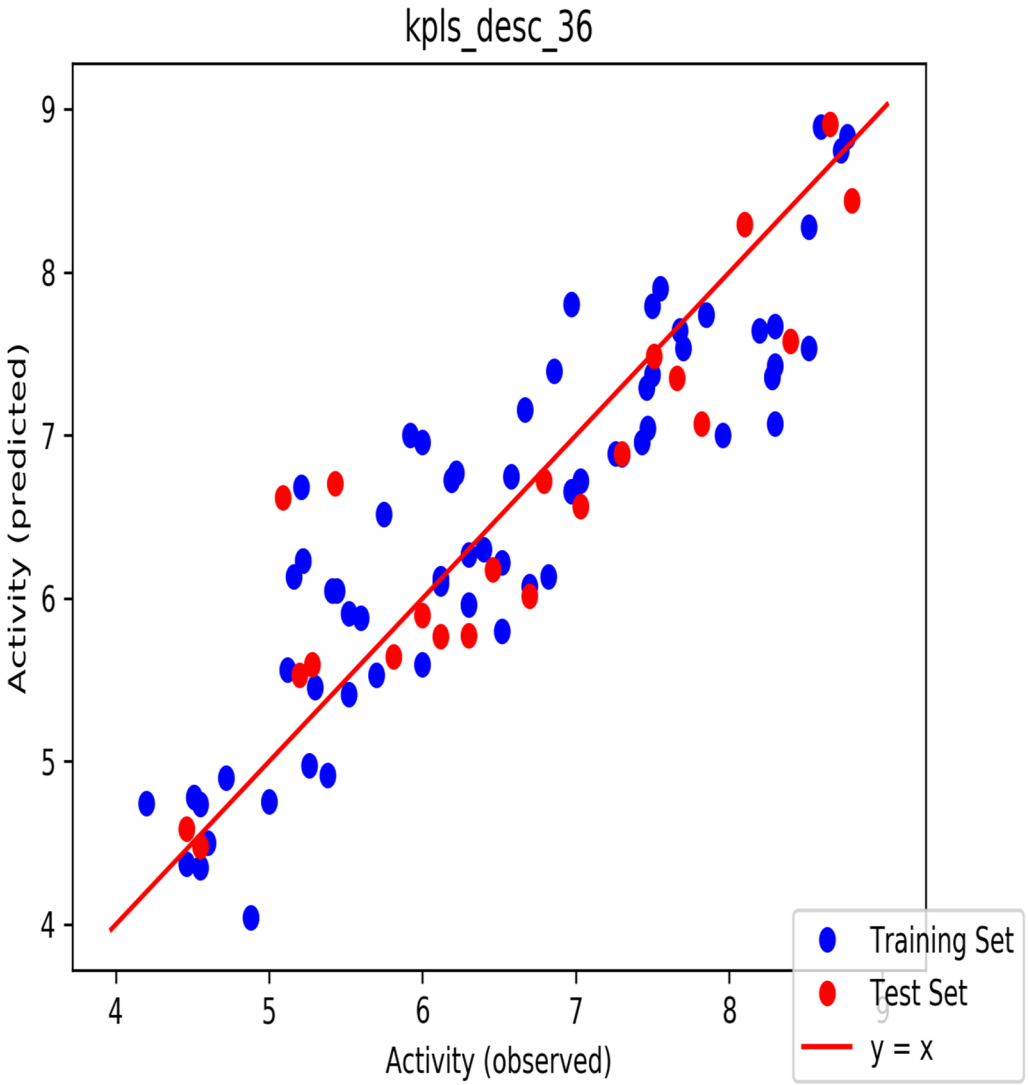


Fig. 14 Correlation between the observed pIC50 and the predicted pIC50 depicted by regression plot

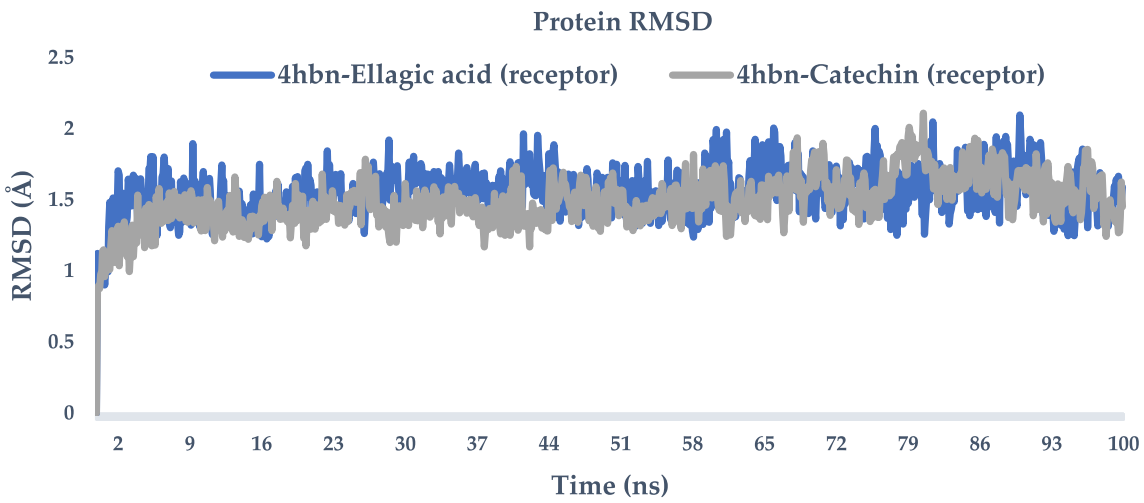


Fig. 15 Protein RMSD plot of simulated complexes {4HBN-ellagic acid in blue, and 4HBN-catechinin in gray}

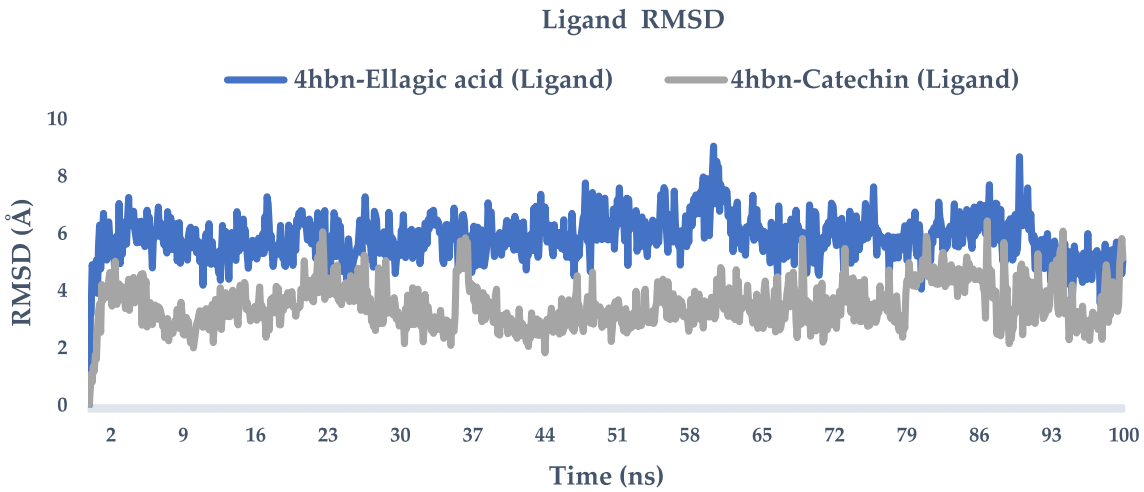


Fig. 16 Ligand RMSD plot of simulated complexes {4HBN-ellagic acid in blue, and 4HBN-catechinin in gray}

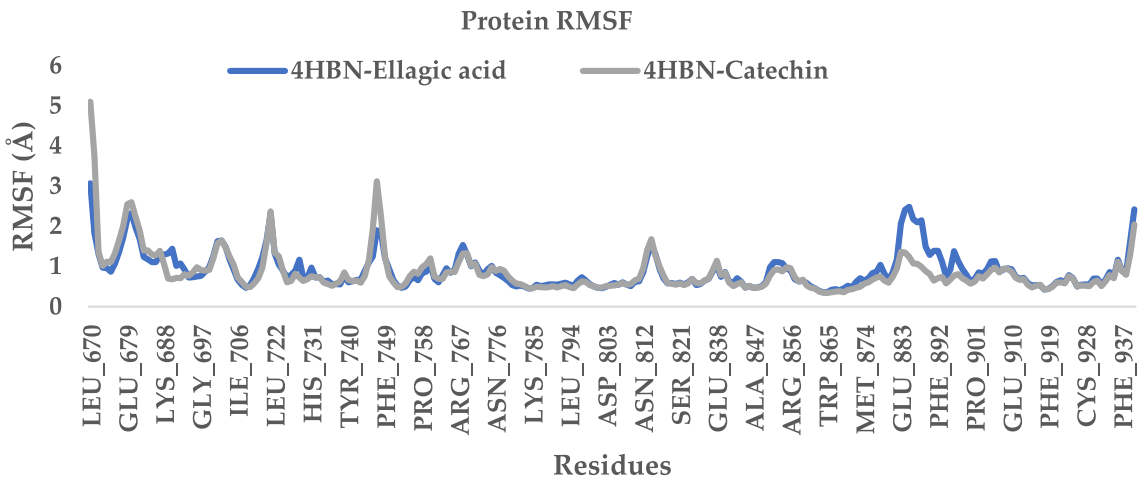


Fig. 17 Protein RMSF plot of simulated complexes {4HBN-ellagicacid in blue, and 4HBN-catechinin gray}

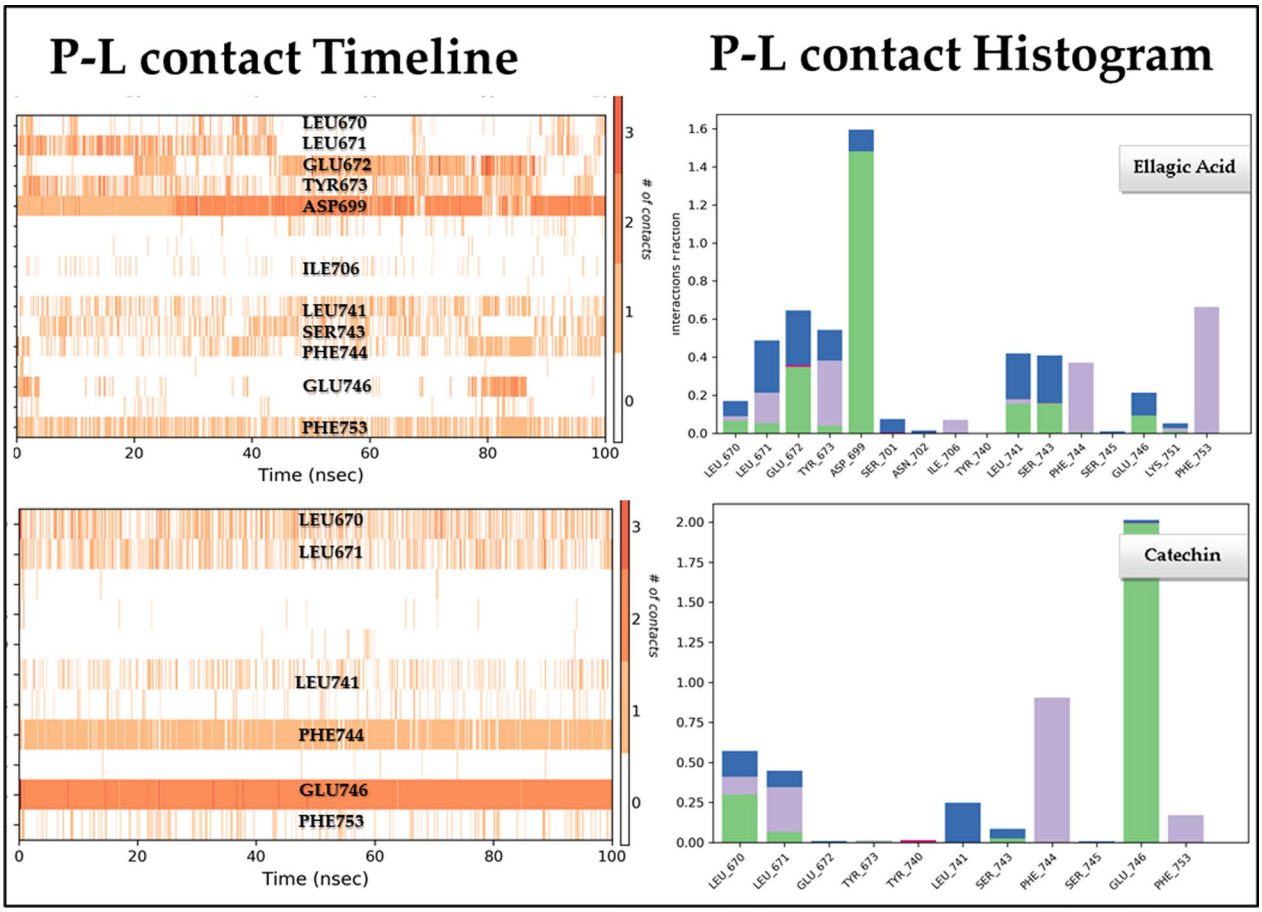


Fig. 18 Protein–ligand contacts of simulated complexes (4HBN complexed with catechin and ellagic acid)—histogram and timeline

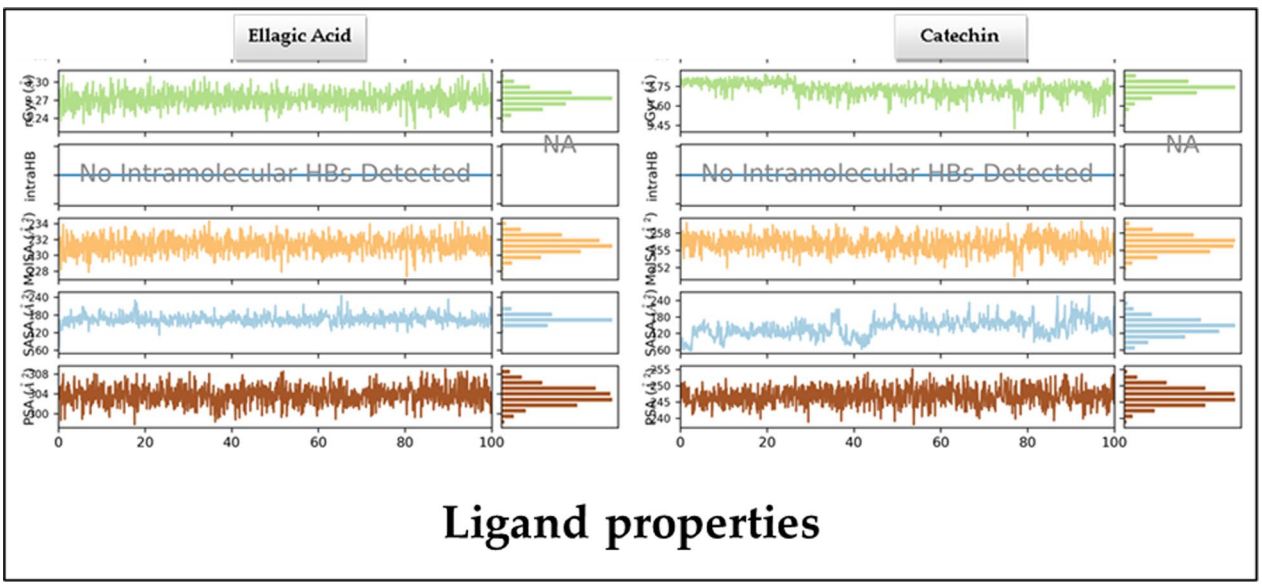


Fig. 19 Ligand properties (RG, SASA, MolSA, PSA) of catechin and ellagic acid in complex with the 4HBN receptor

Acknowledgements
The authors acknowledged the facility support of Teady Bioscience Research Laboratory, Akure, Ondo State.

Author contributions
The concepts and design of the study were contributed by all authors. The following individuals handled the material preparation, data collecting, and analysis: Olusola Olalekan Elekofehinti, Hannah Oluwaseun Popoola, Adedotun Olayemi Oluwatuyi**,** Opeyemi Iwaloye, Moses Orimoloye Akinjiyan, Oluwamodupe Cecilia Ejelonu, Frank Abimbola Ogundolie, Olalekan Isaac Olatunde, and Joao Batista Texeira Rocha. Olusola Olalekan Elekofehinti wrote the original draft of the manuscript, and all authors provided feedback on previous drafts. The final manuscript was read and approved by all authors. Oussama Abchir and Samir Chtita carried out investigation and wrote and edited the manuscript.

Funding
The authors did not receive any funding from any funding body or individual for this study.

Availability of data and materials
Available on reasonable request.

Declarations

Ethics approval and consent to participate
Not applicable.

Consent for publication
Not applicable.

Competing interests
The authors declare no competing interest.

Author details
[1]Bioinformatics and Molecular Biology Unit, Department of Biochemistry, Federal University of Technology Akure, P.M.B 704, Akure, Ondo State, Nigeria. [2]Teady Bioscience Laboratory, Akure, Ondo State, Nigeria. [3]Phytomedicine, Molecular Biology and Bioinformatics Laboratory, Department of Chemical Science (Biochemistry Program), Olusegun Agagu University of Science and Technology, Okitipupa, Ondo State, Nigeria. [4]Department of Biotechnology, Baze University, Abuja, Nigeria. [5]Imported Food Unit, National Agency for Food and Drug Administration and Control, Ota, Nigeria. [6]Laboratory of Analytical and Molecular Chemistry, Faculty of Sciences Ben M'Sik, Hassan II University of Casablanca, 7955 Casablanca, Morocco. [7]Biochemical Toxicology Unit, Department of Biochemistry and Molecular Biology, CCNE, Universidade Federal de Santa Maria, Santa Maria, RS 97105-900, Brazil.

Received: 12 April 2024 Accepted: 12 December 2024
Published online: 14 January 2025

References

1. Chinnasamy S, Zameer F, Muthuchelian K (2020) Molecular and biological mechanisms of apoptosis and its detection techniques. J Oncol Sci 6(1):49–64
2. Schram FR, Ng PKL (2012) What is cancer? J Crustac Biol 32(4):665–672
3. El Nachef L, Bouchet A, Bourguignon M, Foray N (2024) When DNA mutations interplay with cellular proliferation: a narrative history of theories of carcinogenesis. Cancers (Basel) 16(11):2104
4. WHO - World Health Organization (2020) GLOBOCAN—colorectal cancer incidence in the world. Glob Cancer Observ 419:1–2
5. Ferlay J, Colombet M, Soerjomataram I, Parkin DM, Piñeros M, Znaor A et al (2021) Cancer statistics for the year 2020: an overview. Int J Cancer 149(4):778–789
6. Xi Y, Xu P (2021) Global colorectal cancer burden in 2020 and projections to 2040. Transl Oncol 14(10):101174
7. Morgan E, Arnold M, Gini A, Lorenzoni V, Cabasag CJ, Laversanne M et al (2023) Global burden of colorectal cancer in 2020 and 2040: incidence and mortality estimates from GLOBOCAN. Gut 72(2):338–344
8. Mármol I, Sánchez-de-Diego C, Dieste AP, Cerrada E, Yoldi MJR (2017) Colorectal carcinoma: a general overview and future perspectives in colorectal cancer. Int J Mol Sci 18(1):197
9. Pretzsch E, Bösch F, Neumann J, Ganschow P, Bazhin A, Guba M et al (2019) Mechanisms of metastasis in colorectal cancer and metastatic organotropism: hematogenous versus peritoneal spread. J Oncol 2019:7407190
10. Koveitypour Z, Panahi F, Vakilian M, Peymani M, Seyed Forootan F, Nasr Esfahani MH et al (2019) Signaling pathways involved in colorectal cancer progression. Cell Biosci 9(1):97
11. Krall AS, Xu S, Graeber TG, Braas D, Christofk HR (2016) Asparagine promotes cancer cell proliferation through use as an amino acid exchange factor. Nat Commun 7:1–3
12. Nguyen LH, Goel A, Chung DC (2020) Pathways of colorectal carcinogenesis. Gastroenterology 158(2):291–302
13. Malki A, Elruz RA, Gupta I, Allouch A, Vranic S, Al Moustafa AE (2021) Molecular mechanisms of colon cancer progression and metastasis: recent insights and advancements. Int J Mol Sci 22:1–24
14. Heppner DE, Eck MJ (2021) A structural perspective on targeting the <scp>RTK</scp> /Ras/ <scp>MAP</scp> kinase pathway in cancer. Protein Sci 30(8):1535–1553
15. Hattori K, Naguro I, Runchel C, Ichijo H (2009) The roles of ASK family proteins in stress responses and diseases. Cell Commun Signal 7(1):9. https://doi.org/10.1186/1478-811X-7-9
16. Papatsirou M, Artemaki PI, Karousi P, Scorilas A, Kontos CK (2021) Circular RNAs: emerging regulators of the major signaling pathways involved in cancer progression. Cancers (Basel) 13(11):2744
17. Han T, Gao J, Wang L, Qu Y, Sun A, Peng K, et al (2020) Original Article ASK1 inhibits proliferation and migration of lung cancer cells via inactivating TAZ. Am J Cancer Res 10. Available from: www.ajcr.us/
18. Nadel G, Maik-Rachline G, Seger R (2023) JNK cascade-induced apoptosis—a unique role in GqPCR signaling. Int J Mol Sci 24(17):13527
19. Dyari HRE, Rawling T, Chen Y, Sudarmana W, Bourget K, Dwyer JM et al (2017) A novel synthetic analogue of ω-3 17,18-epoxyeicosatetraenoic acid activates TNF receptor-1/ASK1/JNK signaling to promote apoptosis in human breast cancer cells. FASEB J 31(12):5246–5257
20. Yin M, Zhou HJ, Zhang J, Lin C, Li H, Li X, et al (2017) ASK1-dependent endothelial cell activation is critical in ovarian cancer growth and metastasis. JCI Insight 2(18)
21. Luo Y, Gao S, Hao Z, Yang Y, Xie S, Li D et al (2016) Apoptosis signal-regulating kinase 1 exhibits oncogenic activity in pancreatic cancer. Oncotarget 7(46):75155–75164
22. Hayakawa Y, Hirata Y, Sakitani K, Nakagawa H, Nakata W, Kinoshita H et al (2012) Apoptosis signal-regulating kinase-1 inhibitor as a potent therapeutic drug for the treatment of gastric cancer. Cancer Sci 103(12):2181–2185
23. Ogier JM, Nayagam BA, Lockhart PJ (2020) ASK1 inhibition: a therapeutic strategy with multi-system benefits. J Mol Med 98(3):335–348
24. Bahar ME, Kim HJ, Kim DR (2023) Targeting the RAS/RAF/MAPK pathway for cancer therapy: from mechanism to clinical studies. Signal Transduct Target Ther 8(1):455
25. Blondy S, David V, Verdier M, Mathonnet M, Perraud A, Christou N (2020) 5-Fluorouracil resistance mechanisms in colorectal cancer: from classical pathways to promising processes. Cancer Sci 111(9):3142–3154
26. Kadoyama KM (2012) Adverse event profiles of 5-fluorouracil and capecitabine: data mining of the public version of the FDA Adverse Event Reporting System, AERS, and reproducibility of clinical observations. Int J Med Sci 9(1):33–39
27. Bolat E, Sarıtaş S, Duman H, Eker F, Akdaşçi E, Karav S et al (2024) Polyphenols: secondary metabolites with a biological impression. Nutrients 16(15):2550
28. Mondal A, Bhar R, Sinha SN (2021) Ethnomedicinal value and Biological Activities of Spondias mombin L-A Concise Review. Asian Res J Curr Sci 3:87–94
29. Pariyar D, Miya MS, Adhikari A (2021) J Med Herbs 12(2):85–92
30. Bicas JL, Neri-Numa IA, Ruiz ALTG, De Carvalho JE, Pastore GM (2011) Evaluation of the antioxidant and antiproliferative potential of bioflavors. Food Chem Toxicol 49(7):1610–1615

31. Metibemu DS, Akinloye OA, Akamo AJ, Okoye JO, Ojo DA, Morifi E et al (2020) Carotenoid isolates of Spondias mombin demonstrate anticancer effects in DMBA-induced breast cancer in Wistar rats through X-linked inhibitor of apoptosis protein (XIAP) antagonism and anti-inflammation. J Food Biochem 44(12):1–17
32. Cabral B, Siqueira EMS, Bitencourt MAO, Lima MCJS, Lima AK, Ortmann CF et al (2016) Phytochemical study and anti-inflammatory and antioxidant potential of Spondias mombin leaves. Rev Bras 26(3):304–311
33. Sinan KI, Zengin G, Zheleva-Dimitrova D, Gevrenova R, Picot-Allain MCN, Dall'Acqua S et al (2021) Exploring the chemical profiles and biological values of two spondias species (S. dulcis and S. mombin): valuable sources of bioactive natural products. Antioxidants 10(11):1771
34. Maestro. Schrödinger Release 2021–2, Maestro. Schrödinge (LLC): New York, NY. 2021
35. Singh O, Shillings A, Craggs P, Wall I, Rowland P, Skarzynski T et al (2013) Crystal structures of ASK1-inhibtor complexes provide a platform for structure-based drug design. Protein Sci 22(8):1071–1077
36. Schrödinger LNYNYI. Schrödinger Release 2021–3. Protein Preparation Wizard; Epik, . Schrödinger 2021; Prime, Sch (New York, NY): LLC,. 2021
37. Iwaloye O, Elekofehinti OO, Momoh AI, Babatomiwa K, Ariyo EO (2020) In silico molecular studies of natural compounds as possible anti-Alzheimer's agents: ligand-based design. Netw Model Anal Health Inform Bioinform 9(1):1–4
38. Olsson MHM, SØndergaard CR, Rostkowski M, Jensen JH (2011) PROPKA3: consistent treatment of internal and surface residues in empirical p K a predictions. J Chem Theory Comput 7(2):525–537
39. Force Fields. Schrödinger Release 2024–3. Schrödinger, LLC, New York, NY (2024)
40. : LigPrep. Schrödinger Release 2024–3. Schrödinger, LLC, New York, NY (2024)
41. Zhang W, Yang R, Cieplak P, Luo R, Lee T, Caldwell J et al (2003) A point-charge force field for molecular mechanics simulations of proteins based on condensed-phase. J Comput Chem 24(16):1999
42. Duan J, Sastry M, Dixon SL, Lowrie JF, Sherman W (2011) Analysis and comparison of 2D fingerprints: Insights into database screening performance using eight fingerprint methods. J Cheminform 3(SUPPL. 1):2946
43. Elekofehinti OO, Iwaloye O, Josiah SS, Lawal AO, Akinjiyan MO, Ariyo EO (2021) Molecular docking studies, molecular dynamics and ADME/tox reveal therapeutic potentials of STOCK1N-69160 against papain-like protease of SARS-CoV-2. Mol Divers 25(3):1761–1773
44. Sun H, Li Y, Shen M, Tian S, Xu L, Pan P et al (2014) Assessing the performance of MM/PBSA and MM/GBSA methods. 5. Improved docking performance using high solute dielectric constant MM/GBSA and MM/PBSA rescoring. Phys Chem Chem Phys 16(40):22035–22045
45. Guedes IA, de Magalhães CS, Dardenne LE (2014) Receptor-ligand molecular docking. Biophys Rev 6(1):75–87
46. Dixon SL, Duan J, Smith E, Von Bargen CD, Sherman W, Repasky MP (2016) AutoQSAR: an automated machine learning tool for best-practice quantitative structure-activity relationship modeling. Future Med Chem 8(15):1825–1839
47. De Oliveira MT, Katekawa E (2018) On the virtues of automated quantitative structure-activity relationship: the new kid on the block. Future Med Chem 10(3):335–342
48. Rossafi B, Outahar F, Hammoudan I, Moumou M, Touti R, Benharref A et al (2025) Mechanism and stereoselectivity of epoxidation reaction of a β-himachalene derivative: insights from DFT, molecular docking, ADMET, and molecular dynamics investigations. J Mol Struct 1320:139664
49. Abchir O, Daoui O, Nour H, Yamari I, Elkhattabi S, Errougui A et al (2023) Exploration of Cannabis constituents as potential candidates against diabetes mellitus disease using molecular docking, dynamics simulations and ADMET investigations. Sci Afr 21:e01745
50. Chtita S, Fouedjou RT, Belaidi S, Djoumbissie LA, Ouassaf M, Qais FA et al (2022) In silico investigation of phytoconstituents from Cameroonian medicinal plants towards COVID-19 treatment. Struct Chem 33(5):1799–1813
51. Nour H, Yamari I, Abchir O, Mounadi N, Samadi A, Belaidi S et al (2024) Exploring cannabis sativa L for anti-alzheimer potential: an extensive computational study including molecular docking. Mol Dyn ADMET Assessm. https://doi.org/10.21203/rs.3.rs-3986384/v1
52. Khedraoui M, Nour H, Yamari I, Abchir O, Errougui A, Chtita S (2023) Design of a new potent Alzheimer's disease inhibitor based on QSAR, molecular docking and molecular dynamics investigations. Chem Phys Impact 7:100361
53. Yamari I, Abchir O, Siddique F, Zaki H, Errougui A, Talbi M et al (2024) The anticoagulant potential of Lippia Alba extract in inhibiting SARS-CoV-2 Mpro: density functional calculation, molecular docking analysis, and molecular dynamics simulations. Sci Afr 23:e01986
54. Chtita S, Belhassan A, Aouidate A, Belaidi S, Bouachrine M, Lakhlifi T (2021) Discovery of potent SARS-CoV-2 inhibitors from approved antiviral drugs via docking and virtual screening. Comb Chem High Throughput Screen 24(3):441–454
55. Abchir O, Yamari I, Nour H, Daoui O, Elkhattabi S, Errougui A et al (2023) Structure-based virtual screening, ADMET analysis, and molecular dynamics simulation of moroccan natural compounds as candidates α-amylase inhibitors. ChemistrySelect 8(26):e202301092
56. Balogun TA, Chukwudozie OS, Ogbodo UC, Junaid IO, Sunday OA, Ige OM et al (2022) Discovery of putative inhibitors against main drivers of SARS-CoV-2 infection: insight from quantum mechanical evaluation and molecular modeling. Front Chem 11:10
57. Omoboyowa DA, Iqbal MN, Balogun TA, Bodun DS, Fatoki JO, Oyeneyin OE (2022) Inhibitory potential of phytochemicals from Chromolaena odorata L. against apoptosis signal-regulatory kinase 1: a computational model against colorectal cancer. Comput Toxicol 23:100235
58. Ahmad R, Singh J, Wunnava A, Al-Obeed O, Abdulla M, Srivastava S (2021) Emerging trends in colorectal cancer: dysregulated signaling pathways (Review). Int J Mol Med 47(3):14
59. Hayakawa R, Hayakawa T, Takeda K, Ichijo H (2012) Therapeutic targets in the ASK1-dependent stress signaling pathways. Proc Jpn Acad Ser B 88(8):434–453
60. Metibemu DS, Akinloye OA, Akamo AJ, Okoye JO, Ojo DA, Morifi E et al (2020) Carotenoid isolates of Spondias mombin demonstrate anticancer effects in DMBA-induced breast cancer in Wistar rats through X-linked inhibitor of apoptosis protein (XIAP) antagonism and anti-inflammation. J Food Biochem 44(12):e13523
61. Corradi V, Sejdiu BI, Mesa-Galloso H, Abdizadeh H, Noskov SY, Marrink SJ et al (2019) Emerging diversity in lipid-protein interactions. Chem Rev 119(9):5775–5848
62. Murmu S, Archak S (2024) In-silico study of protein-protein interactions in wheat blast using docking and molecular dynamics simulation approach. J Biomol Struct Dyn 42(11):5747–5757
63. Kola I, Landis J (2004) Can the pharmaceutical industry reduce attrition rates? Nat Rev Drug Discov 3(8):711–716
64. Chang Y, Hawkins BA, Du JJ, Groundwater PW, Hibbs DE, Lai F (2022) A guide to in silico drug design. Pharmaceutics 15(1):49
65. Cournia Z, Allen B, Sherman W (2017) relative binding free energy calculations in drug discovery: recent advances and practical considerations. J Chem Inf Model 57(12):2911–2937

Publisher's Note

Springer Nature remains neutral with regard to jurisdictional claims in published maps and institutional affiliations.